International Journal of Robust and Nonlinear Control / Volume 33, Issue 18 / p. 11036-11061

RESEARCH ARTICLE | Full Access

Nonconservative adaptive practical predefined-time sliding mode tracking of uncertain robotic manipulators

Huayang Sai, Zhenbang Xu, Jingkai Cui

First published: 06 August 2023
https://doi-org.fgul.idm.oclc.org/10.1002/rnc.6930
Citations: 1

Abstract

In this article, a nonconservative predefined-time sliding mode control (SMC) scheme and an adaptive practical predefined-time SMC scheme are proposed for trajectory tracking of uncertain robotic manipulators. The nonconservative predefined-time SMCer can achieve strong predefined-time stability of a class of second-order systems without dynamic uncertainties and disturbances. Nonetheless, even in the dynamic uncertainties and disturbances, we show that the studied scheme provides a nonconservative upper bound of settling time. Moreover, considering the unknown coupling uncertainty of the robotic system, adaptive laws are proposed to estimate the upper bound of the coupling uncertainty. Based on the proposed practical predefined-time stability criterion, the designed adaptive practical predefined-time SMCer is shown that the tracking error of the system can converge to a neighborhood of the origin within a predefined time, and the proposed controller weakens the chattering and no prior knowledge of the upper bound of the system uncertainty is required. Several simulation examples are conducted to show the feasibility of the proposed controller, especially evaluating the robustness and the nonconservative settling time.

1 INTRODUCTION

Tracking control of robotic manipulators has always been a challenging topic, aiming at higher tracking accuracy, faster tracking rate, stronger robustness, and anti-interference performance. Among various advanced control methods, sliding mode control (SMC) has attracted scholars' extensive attention due to its ability to withstand bounded external interference and strong robustness.[1, 2] The main point of SMC is to drive and maintain the system state on a stable sliding manifold designed a priori in the state space.[3] To achieve the finite-time convergence, finite-time SMC provides an effective solution for the tracking control of the robotic manipulators, due to its fast transient response and high-precision position tracking performance.[4]

In spite of that, the convergence time of finite-time SMC is an unbound function related to the initial states of the system. Therefore, the application of finite-time SMC is constrained when the initial states of the system are unknown or difficult to obtain. To settle this problem, the fixed-time control technology was developed,[5] which can guarantee a bounded settling time independent of initial states. Several mathematical theories on fixed-time stability have been analyzed[6, 7] and corresponding techniques for fixed-time SMC have been proposed.[8, 9] These concepts have gained widespread attention in the control of robotic manipulators' trajectory tracking, with numerous studies confirming their effectiveness.[10-12]

Compared with finite-time SMC, fixed-time SMC has a remarkable advantage in the settling time of the system, but it is often complex to determine the direct relationship between the control parameters and the settling time. To address this issue, a more advanced concept called predefined-time control was proposed,[13] which provides advanced stability features for the controlled system, such that, the upper bound for settling time of the system can be easily ascertained by tuning parameters, thus providing high determinacy on the system behavior. In some recent works,[14-17] the predefined-time control was utilized in combination with the SMC method to improve the robustness for first-order systems, but these controllers only consider the predefined-time stability in the reaching phase. Furthermore, some works[18-23] made an attempted to extend the predefined-time stability to second-order dynamic systems, even high-order systems.[24, 25] In the work of Sánchez-Torres et al.[18] and Aldana-López et al.,[19] the predefined-time SMCers for the second-order system can guarantee the predefined-time convergence of the reaching phase and the sliding phase, but their upper bounds of settling time are often too conservative. For the robotic system with strict time constraints, the convergence time of its trajectory tracking is designed in advance to avoid conflicts between decoupled task constraints. In recent studies,[26-30] some predefined-time controllers were designed for robotic systems. The controller in the work of Obregon-Flores et al.[30] for redundant manipulators required the acceleration of joints, and the controller in the work of Munoz-Vazquez et al.[27] only achieved the predefined-time convergence in the reaching phase. For these control schemes, too conservative settling-time parameters can result in premature convergence of the system state, which means a waste of system energy consumption and may result in saturation of the actuator. In the works of Pal et al.[31] and Gómez-Gutiérrez et al.,[32] the settling-time conservation was investigated, but the convergence was an exponentially growing for negative state initial values,[31] and the external disturbances of the system were not considered.[32]

In addition, considering the uncertainty in the second-order system, all the above-mentioned predefined-time SMC schemes[18-21, 27] assumed a priori knowledge of the upper bound of the system uncertainty. Obtaining the exact value of the coupling uncertainty poses a challenge in practical applications due to the robotic manipulator's structural complexity and external disturbances. Overcompensating for the uncertainty leads to chattering, which can harm control over the manipulation. Neural networks or fuzzy controls are used to deal with unknown robotic dynamics. However, they require a substantial number of gain parameters, which need adjustment and impose a heavy computational burden on the controller.[33-35] Despite the application of adaptive techniques to finite-time or fixed-time control to resolve the identified issues,[36, 37] the current predefined-time stability criterion's strictness prevents it from satisfying

its prerequisites in conjunction with adaptive techniques. Thus, further research is necessary to address the predefined-time stability criterion for addressing the challenges posed by systems with uncertain parameters.

The article focuses on the problem that the upper bound of the settling time is too conservative and the upper bound of the coupling uncertainty is difficult to obtain in the predefined-time SMC for robotic manipulators. To tackle these challenges, we concentrate on developing an adaptive predefined-time SMC scheme. Our control scheme is based on recent research results on a second-order SMCer with predefined-time convergence in the work of Sánchez-Torres et al.[18] and the settling time estimate of a class of fixed-time stable systems in the work of Aldana-López et al.[19] Their theoretical frameworks allow us to propose a more nonconservative predefined-time SMC scheme for second-order systems, which can guarantee strong predefined-time stability without considering disturbances. To highlight our contributions, we will compare the results of some second-order predefined-time control schemes in recent years.[18-20, 38] Furthermore, a practical predefined-time stability criterion and adaptive laws for the proposed predefined-time SMCer are proposed to guarantee the practical predefined-time stability of the system and to estimate the upper bound of the coupling uncertainty. To illustrate the robustness of our approach in the tracking control of the robotic manipulator, different external disturbances and manipulator structures are simulated, and the numerical simulation results verify the advantages of the proposed control scheme in terms of nonconservative and chattering suppression.

The paper will proceed as follows: we present problem formulation and preliminaries in Section 2. Section 5 details the proposed control scheme. Simulation results of various robotic manipulator designs subjected to external disturbances are presented in Section 9. We proceed to compare our approach with other existing SMC schemes in Section 12 and end by summarizing some closing remarks in Section 13.

2 PRELIMINARIES

2.1 Predefined-time stable systems

Consider the following autonomous dynamical system

$$\dot{x} = fx, \rho, \tag{1}$$

where $x \in \mathbb{R}^n$ denotes the system state, and the vector $\rho \in \mathbb{R}^b$ is the constant parameters of system (1). The function $f : \mathbb{R}^n \to \mathbb{R}^n$ stands for a nonlinear function, with $f0; \rho = 0$. The initial condition of this system is $x_0 = x0 \in \mathbb{R}^n$.

Definition 1. (fixed-time stability[5]) If the origin of system (1) is globally finite-time stable and the settling-time function $T: \mathbb{R}^n \to \mathbb{R}_+ \cup 0$ is bounded, then the system (1) is fixed-time stable.

Definition 2. (settling-time set[14]) If the origin is fixed-time stable for the system (1), then the set of all the bounds of the settling-time function can be defined as
$\mathcal{T} = T_{\max} \in \mathbb{R}_+ : Tx_0 \leqslant T_{\max}, \forall x_0 \in \mathbb{R}^n$.

Remark 1. The above definitions show that the settling time of the finite-time stable system depends on its initial state, and the settling time bound of the fixed-time stable system is a constant. However, in some engineering applications, such as state forecasting, trajectory tracking, etc., the states of the system (1) can reach the origin within the settling time $T_c \in \mathcal{T}$. The settling time is expected to be defined bring forward as a function of the system parameters $T_c = T_c\rho$. In this case, this demand motivates the definition of predefined-time stability.

Definition 3. (predefined-time stability[13]) For the system vector ρ and a predefined-time constant $T_c := T_c\rho > 0$, the origin of system (1) is noted as

(i) If the system (1) is fixed-time stable and the settling-time function $T: \mathbb{R}^n \to \mathbb{R}$ is such that $Tx_0 \leqslant T_c, \forall x_0 \in \mathbb{R}^n$, the system (1) is globally weakly predefined-time stable, and T_c is the weak predefined time.

(ii) If the system (1) is fixed-time stable and the settling-time function $T : \mathbb{R}^n \to \mathbb{R}$ is such that $\sup_{x_0 \in \mathbb{R}^n} Tx_0 = T_c$, the system (1) is globally strongly predefined-time stable, and T_c is the strong predefined time.

The following theorems describe a class of Lyapunov-like conditions for characterizing predefined-time stability.

Lemma 1. (see the works of Sánchez-Torres et al.[18, 39]) *Consider a continuous radially unbounded function $V : \mathbb{R}^n \to \mathbb{R}$ that satisfies*

(i) $Vx = 0$ if and only if $x = 0$.

(ii) $Vx \geqslant 0$ and,

(iii) any solution xt of (1) satisfies

$$\dot{V}x \leqslant -\frac{\alpha^{\frac{\beta q-1}{p}}\Gamma\frac{1-\beta q}{p}}{pT_c}\exp\alpha Vx^p Vx^{\beta q} \tag{2}$$

for $x \in \mathbb{R}^n \setminus \{0\}$ and constants $T_c := T_c\rho > 0, \alpha > 0, \beta > 0, p > 0, q > 0$ such that $0 < \beta q < 1$. $\Gamma\cdot$ is the gamma function.

In this case, the origin of system (1) is called predefined-time stable and T_c is a predefined time.

Lemma 2. (see the work of Aldana-López[19]) *If there is a continuous positive definite radially unbounded function $V : \mathbb{R}^n \to \mathbb{R}$ that satisfies*

$$\dot{V}x \leqslant -\frac{\gamma}{T_c}\alpha Vx^p + \beta Vx^{q^\nu}, \tag{3}$$

for $x \in \mathbb{R}^n \setminus \{0\}$ and constants satisfy $\alpha, \beta, p, q, \nu > 0, \nu p < 1, \nu q > 1$. Let ρ be the parameter vector $\rho = \alpha \ \ \beta \ \ p \ \ q \ \ \nu^T \in \mathbb{R}^5$ of (3). Then, the origin $x = 0$ of system (3) is predefined-time stable with the predefined time T_c and the settling-time function satisfies $T_f = \gamma\rho$, where $\gamma\rho$ is defined as

$$\gamma\rho = \frac{\Gamma m_p \Gamma m_q}{\alpha^k \Gamma kq-p} \frac{\alpha^{m_p}}{\beta}, \tag{4}$$

where $m_p = \frac{1-vp}{q-p}$ *and* $m_q = \frac{vq-1}{q-p}$ *are calculated positive parameters*.

Remark 2. If the equality holds in (2) or (3), it has $Tx_0 = T_c$ as $x_0 \to \infty$. Consequently, from Definition 3 (ii), the system (1) is strongly predefined-time stable with a strong predefined time T_c.

Lemma 3. *If there is a continuous radially unbounded function* $V: \mathbb{R}^n \to \mathbb{R}$ *satisfies*

$$\dot{V}x \leqslant -\frac{\alpha^{\frac{\beta q-1}{p}} \Gamma^{\frac{1-\beta q}{p}}}{pT_c} \exp\alpha V x^p V x^{\beta q} + \eta \tag{5}$$

for $x \in \mathbb{R}^n \setminus \{0\}$ *and constants satisfy* $T_c, \alpha, \beta, p, q, \eta > 0$ *and* $0 < \beta q < 1$. *Then, the origin of system (1) is practically predefined-time stable with the predefined time* $\frac{T_c}{1-\phi}$, *where* $0 < \phi < 1$ *is a defined positive constant, and the residual set of the solution of system (1) is given by*

$$x \in Vx \leqslant \frac{\eta}{\phi\xi\alpha}^{\frac{1}{p+\beta q}}. \tag{6}$$

The proof of Lemma 3 is given in "Appendix A".

Remark 3. The concept of "practically" in Lemma 3 implies that the tracking error can converge to the set of residuals of the origin. According to (3) and (5), let $v = 1$, then the predefined-time stability can be regarded as a special case of the practical predefined-time stability with $\eta = 0$, while the range of the solution of system (1) converges to zero.

2.2 Dynamic model of robotic manipulators

Consider a general n-degrees-of-freedom (DOF) rigid robotic manipulator, whose dynamic model can be written as

$$Mq\ddot{q} + Cq, \dot{q}\dot{q} + Gq = \tau + \tau_d, \tag{7}$$

where $q, \dot{q}, \ddot{q}$ represent the position, velocity, and acceleration vector of the robotic manipulator, respectively. $Mq \in \mathbb{R}^{n \times n}$ is the symmetric and positive-definite matrix, $Cq, \dot{q} \in \mathbb{R}^{n \times n}$ is the centrifugal-Coriolis matrix, and $Gq \in \mathbb{R}^n$ is the Cartesian gravitational term. $\tau \in \mathbb{R}^n$ is the joint torque vector, and $\tau_d \in \mathbb{R}^n$ is a vector of unknown but bounded external disturbance.

To track the trajectory and velocity of the robotic manipulator, the position and velocity tracking errors are denoted as

$$\varepsilon_1 = q_d - q, \varepsilon_2 = \dot{q}_d - \dot{q}, \tag{8}$$

where $q_d \in \mathbb{R}^n$ and $\dot{q}_d \in \mathbb{R}^n$ denote the desired trajectory and desired velocity, respectively. It is reasonable to postulate that the dynamics of the robotic manipulator have the following properties in this paper.

Property 1. Generally, the matrices $Mq, Cq, \dot{q}$ and Gq can be written as[40]

$$\begin{aligned} Mq &= M_0 q + \Delta Mq, \\ Cq, \dot{q} &= C_0 q, \dot{q} + \Delta Cq, \dot{q}, \\ Gq &= G_0 q + \Delta Gq, \end{aligned} \tag{9}$$

where $M_0 q, C_0 q, \dot{q}$, and $G_0 q$ are the nominal parts of the model parameters, and $\Delta Mq, \Delta Cq, \dot{q}$, and ΔGq represent the system uncertainties.

Property 2. According to the dynamic model and Property 1, (7) can be written as[37]

$$M_0 q\ddot{q} + C_0 q, \dot{q}\dot{q} + G_0 q = \tau + \rho, \tag{10}$$

where $\rho \in \mathbb{R}^n$ denotes the coupling uncertainty vector of dynamic model, and ρ can be written as

$$\rho = \tau_d - \Delta Mq\ddot{q} - \Delta Cq, \dot{q}\dot{q} - \Delta Gq\,. \tag{11}$$

3 CONTROL DESIGN

3.1 Predefined-time control of uncertain second-order systems

Consider a second-order system in regular from with a bounded disturbance as

$$\begin{aligned} \dot{x}_1 &= x_2, \\ \dot{x}_2 &= u + \Delta, \end{aligned} \tag{12}$$

where $x = x_1, x_2{}^T \in \mathbb{R}^2$ denotes the system state, $u \in \mathbb{R}$ is the control input, and $\Delta \in \mathbb{R}$ is a bounded disturbance that satisfies $|\Delta| \leqslant \delta$ with $\delta \in \mathbb{R}^+$.

Theorem 1. *With $\alpha_1, \beta_1 > 0, 1 < p_1 < 2, q_1 > 2$, a sliding mode variable is selected as*

$$s_a = \left\lfloor x_2 \right\rceil^2 + \frac{2\gamma_1^2}{T_{c1}^2}\alpha_1 \left\lfloor x_1 \right\rceil^{p_1} + \beta_1 \left\lfloor x_1 \right\rceil^{q_1}, \tag{13}$$

where γ_1, m_p, m_q are some constants satisfying $\gamma_1 = \frac{\Gamma m_p \Gamma m_q}{\frac{1}{2}\alpha_1^{\frac{1}{2}} \Gamma \frac{1}{2} q_1 - p_1} \frac{\alpha_1}{\beta_1}^{m_p}$, $m_p = \frac{2-p_1}{2q_1-p_1}$, $m_q = \frac{q_1-2}{2q_1-p_1}$, and $\left\lfloor x \right\rceil^r = |x|^r \operatorname{sign} x$ with $r \in \mathbb{R}^+$. Then, the predefined-time sliding mode surface is represented as

$$s = x_2 + \left\lfloor s_a \right\rceil^{\frac{1}{2}}. \tag{14}$$

Using (13) and (14), the predefined-time controller for system (12) is constructed as

$$\begin{aligned} u = & \frac{|x_2| \frac{\gamma_2}{2^{\beta_2 q_2 - 1}} \exp \frac{\alpha_2}{2^{p_2}} |s|^{2p_2} \left\lfloor s \right\rceil^{2\beta_2 q_2 - 3} - \frac{\gamma_1^2}{2T_{c1}} \alpha_1 p_1 |x_1|^{p_1 - 1} + \beta_1 q_1 |x_1|^{q_1 - 1} x_2}{|s_a|^{\frac{1}{2}} + |x_2|} \\ & - \frac{\gamma_2}{2^{\beta_2 q_2 - 1}} \exp \frac{\alpha_2}{2^{p_2}} |s|^{2p_2} \left\lfloor s \right\rceil^{2\beta_2 q_2 - 3} - k \operatorname{sign} s, \end{aligned} \tag{15}$$

where $\gamma_2 = \alpha_2^{\frac{\beta_2 q_2 - 2}{p_2}} \Gamma\frac{2-\beta_2 q_2}{p_2} / p_2 T_{c2}$, $\alpha_2, \beta_2, p_2, q_2 > 0$ *such that* $\frac{3}{2} < \beta_2 q_2 < 2$. T_{c1} *and* T_{c2} *represent the upper bounds for the settling time of the system (12) in the sliding phase and the reaching phase, respectively.* k *is a constant that satisfies* $k \geqslant \delta$*, which is used to suppress disturbance* Δ*. In particular, if* $x_1 = x_2 = 0$*, then* $u = 0$*. The system (12) closed by control input (15) is globally predefined-time stable with a predefined time* $T_c = T_{c1} + T_{c2}$ *despite the disturbance* Δ*.*

Proof. The stability analysis of the proposed second-order predefined-time SMC can be divided into the reaching phase and the sliding phase.

Reaching phase: The time-derivative of the sliding mode surface s in (14) is

$$\dot{s} = u + \Delta + \frac{|x_2|\, u + \Delta + \frac{\gamma_1^2}{2T_{c1}^2}\alpha_1 p_1 |x_1|^{p_1 - 1} + \beta_1 q_1 |x_1|^{q_1 - 1} x_2}{|s_a|^{\frac{1}{2}}}. \tag{16}$$

To facilitate the proof, define the variables a and η respectively, which can be expressed as $a = \frac{\gamma_1^2}{2T_{c1}^2}\alpha_1 p_1 |x_1|^{p_1 - 1} + \beta_1 q_1 |x_1|^{q_1 - 1} x_2$, $\eta = \frac{\gamma_2}{2^{\beta_2 q_2 - 1}} \exp\frac{\alpha_2}{2^{p_2}} |s|^{2p_2} \left\lfloor s \right\rceil^{2\beta_2 q_2 - 3}$. Then, substituting (15) into (16) leads to

$$\begin{aligned}
\dot{s} &= \frac{|x_2|\eta - a}{|s_a|^{\frac{1}{2}} + |x_2|} + \frac{\frac{|x_2|^2 \eta - |x_2| a}{|s_a|^{\frac{1}{2}} + |x_2|} - |x_2|\eta + a}{|s_a|^{\frac{1}{2}}} - \eta - k\,\mathrm{sign}s + \Delta - \frac{k|x_2|\,\mathrm{sign}s - \Delta|x_2|}{|s_a|^{\frac{1}{2}}} \\
&= \frac{|x_2|\,|s_a|^{\frac{1}{2}}\eta - |s_a|^{\frac{1}{2}} a + |x_2|^2 \eta - |x_2| a + |s_a|^{\frac{1}{2}} + |x_2| - |x_2|\eta + a}{|s_a|^{\frac{1}{2}} + |x_2|\,|s_a|^{\frac{1}{2}}} \\
&\quad - \eta - k\,\mathrm{sign}s + \Delta - \frac{k|x_2|\,\mathrm{sign}s - \Delta|x_2|}{|s_a|^{\frac{1}{2}}} \\
&= -\eta - k\,\mathrm{sign}s + \Delta - \frac{k|x_2|\,\mathrm{sign}s - \Delta|x_2|}{|s_a|^{\frac{1}{2}}}.
\end{aligned} \tag{17}$$

Consider a Lyapunov function candidate as $V_1 = \frac{1}{2}s^2$. Then, for $s \neq 0$, the first time differential of V_1 yields

$$\begin{aligned}
\dot{V}_1 &= s\dot{s} = -\eta s - k|s| + \Delta s - \frac{k|s| - \Delta s|x_2|}{|s_a|^{\frac{1}{2}}} \\
&= -\eta s + 1 + \frac{|x_2|}{|s_a|^{\frac{1}{2}}}\Delta s - k|s|.
\end{aligned} \tag{18}$$

According to $k \geqslant \delta \geqslant |\Delta|$, (18) can be reduced to

$$\begin{aligned}\dot{V}_1 &\leqslant -\eta s + 1 + \frac{|x_2|}{|s_a|^{\frac{1}{2}}}(|\Delta| - k)|s| \\ &\leqslant -\eta s = -\frac{\gamma_2}{2^{\beta_2 q_2 - 1}}\exp\frac{\alpha_2}{2^{p_2}}|s|^{2p_2}\left\lfloor s\right\rceil^{2\beta_2 q_2 - 3}s \\ &= -\frac{\alpha_2^{\frac{\beta_2 q_2 - 2}{p_2}}\Gamma\frac{2-\beta_2 q_2}{p_2}}{p_2 T_{c2}}\exp\frac{\alpha_2}{2^{p_2}}|s|^{2p_2}\frac{|s|^{2\beta_2 q_2 - 1}}{2^{\beta_2 q_2 - 1}} \\ &= -\frac{\alpha_2^{\frac{\beta_2 q_2 - 1 - 1}{p_2}}\Gamma\frac{1-\beta_2 q_2 - 1}{p_2}}{p_2 T_{c2}}\exp\alpha_2 V_1^{p_2} V_1^{\beta_2 q_2 - 1}.\end{aligned} \tag{19}$$

According to $\frac{1}{2} < \beta_2 q_2 - 1 < 1$ and Lemma 1, the origin of system (12) is predefined-time stable in the reaching phase with the predefined time T_{c2}.

Sliding phase: The system state convergence enters the sliding phase once the system state is constrained to the manifold $s = 0$, that is, for $t \geqslant T_{c2}$, the solutions of the system (12) can be written as the following reduced-order dynamics (see Appendix B for the derivation)

$$\dot{x}_1 = x_2 = -\frac{\gamma_1}{T_{c1}}\alpha_1 |x_1|^{p_1} + \beta_1 |x_1|^{q_1}{}^{\frac{1}{2}}\mathrm{sign}x_1. \tag{20}$$

Thus, consider $V_2 = |x_1|$ as a continuous radially unbounded positive definite Lyapunov candidate function, and the first derivative of V_2 leads to

$$\dot{V}_2 = \dot{x}_1\mathrm{sign}x_1 = -\frac{\gamma_1}{T_{c1}}\alpha_1 |x_1|^{p_1} + \beta_1 |x_1|^{q_1}{}^{\frac{1}{2}} = -\frac{\gamma_1}{T_{c1}}\alpha_1 V_2{}^{p_1} + \beta_1 V_2{}^{q_1}{}^{\frac{1}{2}}. \tag{21}$$

Using Lemma 2, the parameter ν should be $\frac{1}{2}$, then it can be concluded that the system (12) is predefined-time stable in the sliding phase with the predefined time T_{c1}.

Therefore, the proposed predefined-time SMCer can achieve predefined-time convergence for arbitrary second-order systems with the predefined time $T_c = T_{c1} + T_{c2}$. This completes our proof.

Remark 4. The definition of the sliding mode variable s_a is conducive to simplifying the structure of the controller and making the proof process of the predefined-time stability of the controller more concise. Based on the designed sliding mode variable s_a, the designed sliding surface s can guarantee the predefined-time stability of the system in the sliding phase.

Remark 5. From (13), we have $|s_a|^{\frac{1}{2}} + |x_2| = 0$ when and only when $|x_1| = |x_2| = 0$. At this time, the system converges to the origin and $u = 0$ can be specified to avoid singularities as declared in Theorem 1.

Example 1. To illustrate Theorem 1, the system (12) with $\Delta = 0$ and the controller in (15) are considered for simulation. The parameters of the proposed controller are set to $\alpha_1 = 4, \beta_1 = \frac{1}{4}, q_1 = 3, p_1 = 1.5, p_2 = \beta_2 = 1, \alpha_2 = 10^{-3}, q_2 = 1.75$. The trajectories of the system

are simulated with different initial states and different predefined-time parameters in Figure 1. It can be seen $\sup_{x0 \in \mathbb{R}} Tx_0 = T_c$ as stated in Theorem 1.

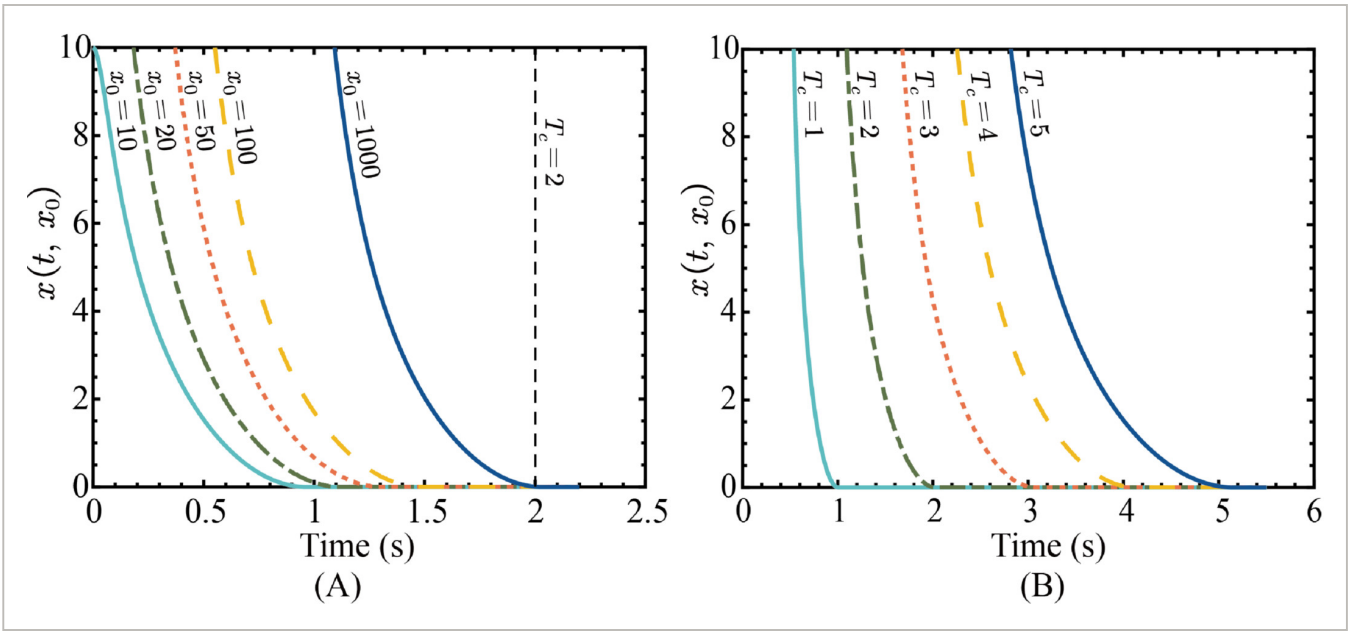

FIGURE 1

Open in figure viewer | PowerPoint

State trajectories of a second-order system with the controller (15). (A) $T_c = 2T_{c1} = 2T_{c2} = 2$ and different initial states $x_0 = 10, 20, 50, 100, 1000$. (B) $x_0 = 1000$ and different predefined-time $T_c = 2T_{c1} = 2T_{c2} = 1, 2, 3, 4, 5$.

Remark 6. Due to the presence of disturbance, the system may converge to the origin before T_c even if $|x_0|$ tends to infinity. In other words, if the disturbance is present, the origin of the system (12) is globally weakly predefined-time stable as per Definition 3 (i). According to Definition 3 (ii), if $\Delta = k\text{sign}s$, then the origin of system (12) is globally strongly predefined-time stable with T_c being the least upper bound of the settling time; However, such a condition cannot be achieved in practical scenarios.

Remark 7. If the described second-order system (12) is undisturbed, that is $\Delta = k = 0$, then it is easy to see that (19) is an equation. Using Definition 3 (ii), the origin of system (12) without disturbance is globally strongly predefined-time stable. If the system contains disturbances, then according to Definition 3 (i), it can be obtained that the origin of the system (12) is globally weakly predefined-time stable.

Example 2. A comparison of the proposed method with some predefined-time control schemes[18-20, 38] is shown in Figure 2. Our proposed control input u is given in (15), and the same parameters as in example 1 are applied to the second-order system (12) with $\Delta = 0$. It follows from Theorem 1 that, with $T_{c1} = T_{c2} = 1$, the second-order system is globally predefined-time stable with the predefined time $T_c = 2$. To make a fair comparison of the control performances, control schemes[18-20, 38] are designed with the same predefined time $T_c = 2$, and other control parameters are consistent with the reference values given in the literature.

From Figure 2, it can be obtained that, with $x_0 = 100$, the upper bound for the settling time of the existing predefined-time control schemes[19, 20, 38] is much more conservative than our approach. For the control scheme in the work of Sánchez-Torres et al.,[18] due to the $\exp|x_1|^{p_1}$ term in the sliding mode surface, it will produce an explosive increase as the x_0 increases. It can be clearly seen that, with $x_0 = 10$, the upper bound for the settling time of control scheme in the work of Sánchez-Torres et al.[18] is more conservative than our approach.

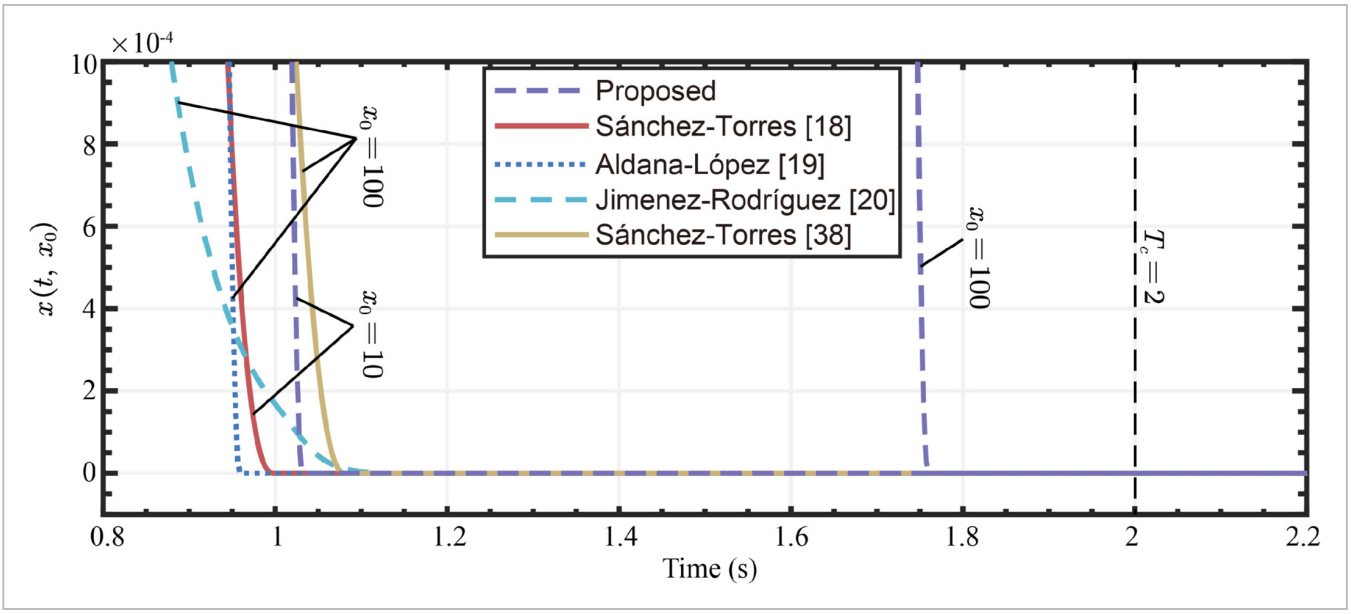

FIGURE 2

Open in figure viewer | PowerPoint

State trajectories of a second-order system with the predefined time $T_c = 2$ s.

The proposed predefined-time control scheme for a second-order system without disturbance is unscaled in the proof process of predefined time stability, unlike other control schemes,[18-20, 38] leading to a less conservative upper bound on settling time. As a result, the settling time of the proposed scheme is closer to the predefined time parameters, implying a more reasonable predefined convergence time. A less conservative settling time function is preferable for promoting a reasonable predefined-time convergence. Conversely, a conservative upper bound on settling time implies a faster convergence rate, which often leads to greater control input and increased energy consumption.

3.2 Predefined-time sliding mode tracking control for uncertain robotic manipulators

According to the dynamic model of robotic manipulators in (7)-(11), the dynamic errors of the rigid manipulators can be rewritten as

$$\begin{aligned} \dot{\varepsilon}_1 &= \varepsilon_2 \\ \dot{\varepsilon}_2 &= M_0^{-1}q - C_0 q, \dot{q} - G_0 q - M_0 q \ddot{q}_d + \tau + \rho \end{aligned} \quad (22)$$

Then, (22) can be rewritten as the following form

$$\begin{aligned}\dot{\varepsilon}_1 &= \varepsilon_2\\ \dot{\varepsilon}_2 &= F\varepsilon_1,\varepsilon_2 + B\varepsilon_1,\varepsilon_2\tau + D\varepsilon_1,\varepsilon_2\end{aligned}, \tag{23}$$

where $F\varepsilon_1,\varepsilon_2 = -M_0^{-1}C_0q,\dot{q} + G_0q - \ddot{q}_d$, $B\varepsilon_1,\varepsilon_2 = M_0^{-1}q$ and $D\varepsilon_1,\varepsilon_2 = M_0^{-1}q\rho = M_0^{-1}q\cdot\tau_d - \Delta Mq\ddot{q} - \Delta Cq,\dot{q}\dot{q} - \Delta Gq$.

Assumption 1. The coupling uncertainty of the robotic manipulator should be bounded, and its upper bound can be constrained to Reference 41

$$|D_i\varepsilon_1,\varepsilon_2| \leqslant \delta_i = b_{0i} + b_{1i}|q_i| + b_{2i}|\dot{q}_i|^2, \tag{24}$$

where $\delta, b_0, b_1, b_2 \in \mathbb{R}^n$ are all positive vectors, and $\delta_i, b_{0i}, b_{1i}, b_{2i}, D_i\varepsilon_1,\varepsilon_2$ are the ith element of vectors δ, b_0, b_1, b_2, and $D\varepsilon_1,\varepsilon_2$, respectively.

Remark 8. In the dynamic control of robotic manipulators, (24) is a common assumption to constrain the coupling uncertainty of the system, such as the work of Boukattata et al.[37] and Yi et al.[42]

Inspired by the predefined-time control scheme for second-order systems proposed in Section 5, the following theorem can be used for predefined-time tracking control of uncertain manipulators.

Theorem 2. *The predefined-time sliding mode variable and sliding mode surface are designed as*

$$\begin{aligned}s_{ai} &= \left\lfloor\varepsilon_{2i}\right\rceil^2 + \frac{\gamma_1^2}{T_{c1}^2}\alpha_1\left\lfloor\varepsilon_{1i}\right\rceil^{p_1} + \beta_1\left\lfloor\varepsilon_{1i}\right\rceil^{q_1},\\ s_i &= \varepsilon_{2i} + \left\lfloor s_{ai}\right\rceil^{\frac{1}{2}},\end{aligned} \tag{25}$$

where $\alpha_1,\beta_1 > 0, 1 < p_1 < 2, q_1 > 2, m_p = \frac{2-p_1}{2q_1-p_1}$, $m_p = \frac{q_1-2}{2q_1-p_1}$, $\gamma_1 = \frac{\Gamma m_p\Gamma m_q}{\alpha_1^{\frac{1}{2}}\Gamma\frac{1}{2}q_1-p_1}\frac{\alpha_1}{\beta_1}^{m_p}$. *The predefined-time SMC scheme for robotic manipulators with bounded coupling uncertainty is designed as*

$$\begin{aligned}\tau_i &= B^{-1}\varepsilon_{1i},\varepsilon_{2i}u_i - F\varepsilon_{1i},\varepsilon_{2i},\\ u_i &= \frac{|\varepsilon_{2i}|\frac{\gamma_2}{2^{\beta_2q_2-1}}\exp\frac{\alpha_2}{2^{p_2}}|s_i|^{2p_2}\left\lfloor s_i\right\rceil^{2\beta_2q_2-3} - \frac{\gamma_1^2}{2T_{c1}}\alpha_1p_1|\varepsilon_{1i}|^{p_1-1} + \beta_1q_1|\varepsilon_{1i}|^{q_1-1}\varepsilon_{2i}}{|s_{ai}|^{\frac{1}{2}} + |\varepsilon_{2i}|}\\ &\quad - \frac{\gamma_2}{2^{\beta_2q_2-1}}\exp\frac{\alpha_2}{2^{p_2}}|s_i|^{2p_2}\left\lfloor s_i\right\rceil^{2\beta_2q_2-3} - k_i\mathrm{sign}s_i,\\ k_i &= b_{0i} + b_{1i}|q_i| + b_{2i}|\dot{q}_i|^2,\end{aligned} \tag{26}$$

where $\alpha_2,\beta_2,p_2,q_2 > 0, \frac{3}{2} < \beta_2q_2 < 2$, $\gamma_2 = \alpha_2^{\frac{\beta_2q_2-2}{p_2}}\Gamma\frac{2-\beta_2q_2}{p_2} / p_2T_{c2}$, T_{c1}, *and* T_{c2} *denote the predefined-time constants in sliding phase and reaching phase, and vectors* b_0, b_1, b_2 *are given positive vectors satisfying (24). Then, dynamic errors of the robotic system are globally predefined-time stable with a predefined time* $T_c = T_{c1} + T_{c2}$.

Proof. The proof is similar to Theorem 1 in Section 5; hence it is omitted here to avoid the repetition of the proof process.

The predefined-time SMC scheme presented here is also applicable to other second-order mechanical systems with bounded disturbances, like inverted pendulum systems and permanent magnet linear motors. Obtaining the upper bounds for these systems is difficult due to model uncertainty and disturbance complexity. An effective way to solve this problem is by using adaptive laws to estimate the upper bounds of system coupling uncertainties.

3.3 Adaptive practical predefined-time sliding mode tracking control for uncertain robotic manipulators

For the dynamic model of robotic manipulators in (23), considering the complexity of the structure of the uncertainties and external disturbances, b_0, b_1, b_2 are often difficult to determine or overestimated to satisfy (24). To surmount the aforementioned weakness, an adaptive practical predefined-time SMC scheme for robotic manipulators is designed as follows.

Theorem 3. *The adaptive practical predefined-time SMC scheme is designed as*

$$\begin{aligned}
\tau_i &= B^{-1}\varepsilon_{1i}, \varepsilon_{2i}u_i - F\varepsilon_{1i}, \varepsilon_{2i}, \\
u_i &= \frac{|\varepsilon_{2i}| \frac{\gamma_2}{2^{\beta_2 q_2 - 1}} \exp \frac{\alpha_2}{2^{p_2}} |s_i|^{2p_2} \left| s_i \right|^{2\beta_2 q_2 - 3} - \frac{\gamma_1^2}{2T_{c1}} \alpha_1 p_1 |\varepsilon_{1i}|^{p_1 - 1} + \beta_1 q_1 |\varepsilon_{1i}|^{q_1 - 1} \varepsilon_{2i}}{|s_{ai}|^{\frac{1}{2}} + |\varepsilon_{2i}|} \\
&\quad - \frac{\gamma_2}{2^{\beta_2 q_2 - 1}} \exp \frac{\alpha_2}{2^{p_2}} |s_i|^{2p_2} \left| s_i \right|^{2\beta_2 q_2 - 3} - k_i \operatorname{sign} s_i, \\
k_i &= \hat{b}_{0i} + \hat{b}_{1i} |q_i| + \hat{b}_{2i} |\dot{q}_i|^2,
\end{aligned} \tag{27}$$

where

$$\alpha_2, \beta_2, p_2, q_2, T_{c2} > 0, 1 < p_1 < 2, q_1 > 2, \frac{3}{2} < \beta_2 q_2 < 2, \gamma_1 = \frac{\Gamma m_p \Gamma m_q}{\frac{1}{\alpha_1^2} \Gamma \frac{1}{2} q_1 - p_1} \frac{\alpha_1}{\beta_1}^{m_p}, \gamma_2 = \alpha_2^{\frac{\beta_2 q_2 - 2}{p_2}} \Gamma \frac{2 - \beta_2 q_2}{p_2} / p_2 T_{c2}$$

. T_{c1} denotes the predefined-time constant in sliding phase, and the sliding mode surface is defined in (25). The estimated parameters $\hat{b}_{0i}, \hat{b}_{1i}$, and $\hat{b}_{2i}$ are updated by the proposed adaptive laws

$$\begin{aligned}
\dot{\hat{b}}_{0i} &= \lambda_0 |s_i| 1 + \frac{|\varepsilon_{2i}|}{|s_{ai}|^{\frac{1}{2}}}, \\
\dot{\hat{b}}_{1i} &= \lambda_1 |s_i| 1 + \frac{|\varepsilon_{2i}|}{|s_{ai}|^{\frac{1}{2}}} |q_i|, \\
\dot{\hat{b}}_{2i} &= \lambda_2 |s_i| 1 + \frac{|\varepsilon_{2i}|}{|s_{ai}|^{\frac{1}{2}}} |\dot{q}_i|^2,
\end{aligned} \tag{28}$$

where $\lambda_i, i = 0, 1, 2$ are defined positive constants. Then, the origin of the robotic system is practically predefined-time stable with a predefined time $\frac{T_{c2}}{1-\phi}$, where $0 < \phi < 1$ is a defined positive constant.

Proof. To make the proof process clearer, the ith elements of control vectors are considered in the proof process. Consider the following Lyapunov function candidate

$$V_3 = \frac{1}{2}s^2 + \sum_{i=0}^{2} \frac{1}{2\lambda_i}\hat{b}_i - b_i^{\ 2}. \tag{29}$$

Combining (17) and (18), it takes the derivative of V_3 with respect to time produces

$$\dot{V}_3 = -\eta s - k \mid s \mid + Ds - \frac{k \mid s \mid - Ds \mid \varepsilon_2 \mid}{\mid s_a \mid^{\frac{1}{2}}} + \sum_{i=0}^{2} \frac{1}{\lambda_i}\hat{b}_i - b_i\dot{\hat{b}}_i. \tag{30}$$

By substituting the adaptive control law (28) into (30), one has

$$\begin{aligned}
\dot{V}_3 &= -\eta s - \hat{b}_0 + \hat{b}_1 \mid q \mid + \hat{b}_2 \mid \dot{q} \mid^2 \mid s \mid + Ds - \frac{\mid \varepsilon_2 \mid}{\mid s_a \mid^{\frac{1}{2}}}\hat{b}_0 + \hat{b}_1 \mid q \mid + \hat{b}_2 \mid \dot{q} \mid^2 \mid s \mid + \frac{\mid \varepsilon_2 \mid}{\mid s_a \mid^{\frac{1}{2}}} Ds \\
&\quad + 1 + \frac{\mid \varepsilon_2 \mid}{\mid s_a \mid^{\frac{1}{2}}} \mid s \mid \hat{b}_0 - b_0 + \hat{b}_1 - b_1 \mid q \mid + \hat{b}_2 - b_2 \mid \dot{q} \mid^2 \\
&= -\eta s - \hat{b}_0 + \hat{b}_1 \mid q \mid + \hat{b}_2 \mid \dot{q} \mid^2 \mid s \mid + Ds - \frac{\mid \varepsilon_2 \mid}{\mid s_a \mid^{\frac{1}{2}}}\hat{b}_0 + \hat{b}_1 \mid q \mid + \hat{b}_2 \mid \dot{q} \mid^2 \mid s \mid + \frac{\mid \varepsilon_2 \mid}{\mid s_a \mid^{\frac{1}{2}}} Ds \\
&\quad + \hat{b}_0 + \hat{b}_1 \mid q \mid + \hat{b}_2 \mid \dot{q} \mid^2 \mid s \mid - b_0 + b_1 \mid q \mid + b_2 \mid \dot{q} \mid^2 \mid s \mid \\
&\quad + \frac{\mid \varepsilon_2 \mid}{\mid s_a \mid^{\frac{1}{2}}}\hat{b}_0 + \hat{b}_1 \mid q \mid + \hat{b}_2 \mid \dot{q} \mid^2 \mid s \mid - \frac{\mid \varepsilon_2 \mid}{\mid s_a \mid^{\frac{1}{2}}} b_0 + b_1 \mid q \mid + b_2 \mid \dot{q} \mid^2 \mid s \mid \\
&= -\eta s + Ds - b_0 + b_1 \mid q \mid + b_2 \mid \dot{q} \mid^2 \mid s \mid + \frac{\mid \varepsilon_2 \mid}{\mid s_a \mid^{\frac{1}{2}}} Ds - \frac{\mid \varepsilon_2 \mid}{\mid s_a \mid^{\frac{1}{2}}} b_0 + b_1 \mid q \mid + b_2 \mid \dot{q} \mid^2 \mid s \mid \\
&\leqslant -\eta s + 1 + \frac{\mid \varepsilon_2 \mid}{\mid s_a \mid^{\frac{1}{2}}} \mid s \mid \mid D \mid - b_0 + b_1 \mid q \mid + b_2 \mid \dot{q} \mid^2 \mid s \mid .
\end{aligned} \tag{31}$$

Let $\Lambda_b = \sum_{i=0}^{2} \frac{1}{2\lambda_i}\hat{b}_i - b_i^{\ 2}$ and considering (19), we can have

$$-\eta s = -\frac{\alpha_2^{\frac{\beta_2 q_2 - 2}{p_2}} \Gamma\frac{2-\beta_2 q_2}{p_2}}{p_2 T_{c2}} \exp\alpha_2 \frac{1}{2}s^2 + \Lambda_b - \Lambda_b^{\ p_2} \frac{1}{2}s^2 + \Lambda_b - \Lambda_b^{\ \beta_2 q_2 - 1}. \tag{32}$$

Then, with $\Lambda_b > 0$ and s being bounded, there must exist a bounded positive constant ξ_b satisfying

$$\begin{aligned}
-\eta s &= -\frac{\alpha_2^{\frac{\beta_2 q_2 - 2}{p_2}} \Gamma\frac{2-\beta_2 q_2}{p_2}}{p_2 T_{c2}} \exp\alpha_2 \frac{1}{2}s^2 + \Lambda_b^{\ p_2} \frac{1}{2}s^2 + \Lambda_b^{\ \beta_2 q_2 - 1} + \xi_b \\
&= -\frac{\alpha_2^{\frac{\beta_2 q_2 - 1 - 1}{p_2}} \Gamma\frac{1-\beta_2 q_2 - 1}{p_2}}{p_2 T_{c2}} \exp\alpha_2 V_3^{p_2} V_3^{\beta_2 q_2 - 1} + \xi_b .
\end{aligned} \tag{33}$$

Substituting (33) into (31) yields

$$\dot{V}_3 \leqslant -\frac{\alpha_2^{\frac{\beta_2 q_2 - 1 - 1}{p_2}} \Gamma^{\frac{1-\beta_2 q_2 - 1}{p_2}}}{p_2 T_{c2}} \exp \alpha_2 V_3^{p_2} V_3^{\beta_2 q_2 - 1} + \xi, \tag{34}$$

where $\xi = \xi_b + 1 + \frac{|\varepsilon_2|}{|s_a|^{\frac{1}{2}}} |s||D| - b_0 + b_1 |q| + b_2 |\dot{q}|^2 |s|$. With $\xi_b > 0, 1 + \frac{|\varepsilon_2|}{|s_a|^{\frac{1}{2}}} |s||D| - b_0 + b_1 |q| + b_2 |\dot{q}|^2 |s| \leqslant 0$, there are two cases should be discussed.

Case 1. If $\xi \leqslant 0$, (34) can be written as

$$\dot{V}_3 \leqslant -\frac{\alpha_2^{\frac{\beta_2 q_2 - 1 - 1}{p_2}} \Gamma^{\frac{1-\beta_2 q_2 - 1}{p_2}}}{p_2 T_{c2}} \exp \alpha_2 V_3^{p_2} V_3^{\beta_2 q_2 - 1}. \tag{35}$$

According to Lemma 1, it can be obtained that the system is predefined-time stable with the settling time T_{c2}. The proof of predefined-time stability in the sliding phase is the same as that in Theorem 1, hence it is omitted here.

Case 2. If $\xi > 0$, combined with $1 + \frac{|\varepsilon_2|}{|s_a|^{\frac{1}{2}}} |s||D| - b_0 + b_1 |q| + b_2 |\dot{q}|^2 |s| \leqslant 0$, we have $\xi \leqslant \xi_b$. Therefore, (34) can be written as

$$\dot{V}_3 \leqslant -\frac{\alpha_2^{\frac{\beta_2 q_2 - 1 - 1}{p_2}} \Gamma^{\frac{1-\beta_2 q_2 - 1}{p_2}}}{p_2 T_{c2}} \exp \alpha_2 V_3^{p_2} V_3^{\beta_2 q_2 - 1} + \xi_b. \tag{36}$$

Combining that ξ_b is a positive constant, and Lemma 3, it can be obtained that the system is practically predefined-time stable and the tracking error can converge to a neighborhood near the origin with the predefined time $\frac{T_{c2}}{1-\phi}$.

This completes our proof.

Compared with the nonadaptive predefined-time controller in Theorem 2, the proposed update laws in (28) are designed to estimate the parameters of the robotic uncertainty bounds, and the estimated results are then used in the predefined-time controller (27) to resist the effects of system uncertainty. Figure 3 shows the control signals flowchart for the proposed adaptive practical predefined-time SMCer in (27) and (28).

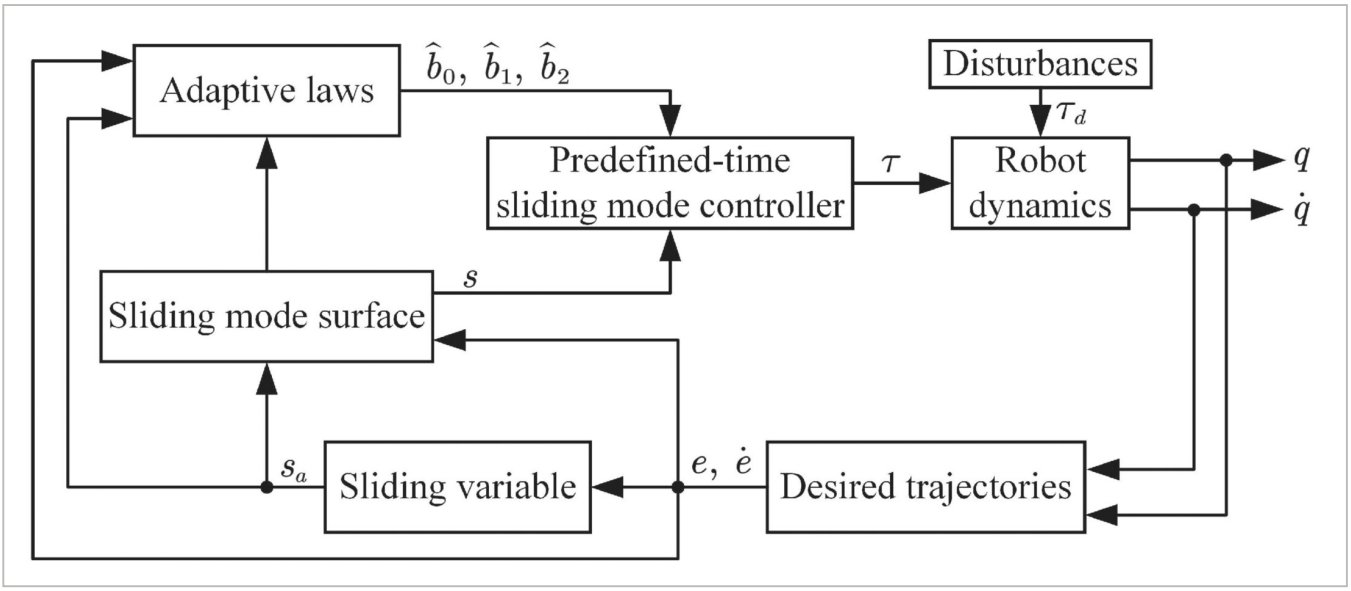

FIGURE 3

Open in figure viewer | PowerPoint

Block diagram showing the flow of the control signals for the adaptive practical predefined-time SMC scheme.

Remark 9. Since the predefined-time stability of the system can be regarded as a special case of the practical predefined-time stability, for ease of expression, we can only declare in this paper that the adaptive controller is practically predefined-time stable.

Remark 10. In contrast to the adaptive update laws currently available for robotic systems,[43-45] the update laws proposed in this research do not need to be derived from the inherent properties of the systems, such as symmetry, antisymmetry, and regression properties. Consequently, the proposed adaptive control scheme may be suitable for a broader range of mechanical systems. Additionally, unlike the predefined-time controller discussed in Section 6, which necessitates the fulfillment of Assumption 1, the proposed adaptive controller is more resilient to external disturbances, such as monotonically increasing bounded disturbances over a short duration.

Remark 11. From the perspective of engineering application, the main factors restricted in robotic dynamics control come from: (i) the uncertainties and external disturbances of the system dynamic model, (ii) the upper bound of the coupling uncertainty of the system is difficult to obtain, (iii) the feasibility of system control input.[37] Obviously, the controller proposed in this paper neither requires the accurate dynamics model, nor does it require the upper bound of the coupling uncertainty. Generally speaking, each joint of a robotic manipulator is installed with an encoder and a tachometer to measure the angle and velocity of the joint. Therefore, the described control scheme is expected to be suitable for actual robotic manipulators.

Remark 12. The main cause of chattering in the system controlled by the proposed controller (27) is the $\lfloor s \rceil^{2\beta_2 q_2 - 3}$ term. To mitigate the chattering effect, the term can be modified using the

common boundary layer technique to $\frac{ss^{2\beta_2 q_2 - 3}}{s + s_0}$ ($s_0 \in \mathbb{R}^+$), or some technologies, such as the time-delay estimation, can be used to attenuate or eliminate the chattering.

Remark 13. Control parameters $q_i, p_i, \alpha_i, \beta_i$, and T_{ci} $i = 1, 2$ should be carefully selected to match the requirements for tracking accuracy and input torque. Parameter q_1 should satisfy $q_1 > 2$. As q_1 increases, it reduces the initial torque chatter of the system. However, increasing it simultaneously diminishes the system's tracking accuracy. Parameter p_1 should satisfy $1 < p_1 < 2$. One should aim to get as close to 1 as possible because the initial torque chatter and steady-state error of the system would rise as p_1 increases. Although the performance of the controller is insensitive to α_1, a large value of this parameter causes chattering of the initial torque of the system. Increasing parameter β_1 can enhance system tracking accuracy. However, it can also cause an early increase in the initial torque, which should be chosen smaller than α_1. Increasing p_2 can improve tracking accuracy and reduce initial system torque, but may also cause tracking error overshoot which should be adjusted p_2 within the range $1 \leqslant p_2 \leqslant 2$. Choose a small value for parameter α_2, as increasing it would lead to an increase in initial torque and system overshoot despite improving system tracking accuracy, and a value of 10^{-3} is generally recommended. Optimal system performance requires that β_2 and q_2 parameters fall within the recommended range of $1.5 < \beta_2 q_2 < 2$. Increasing $\beta_2 q_2$ may decrease tracking error but also raises control torque. The s_0 parameter in Remark 12 should be minimized since doing so can help reduce system chattering, but increasing s_0 has the negative consequence of increasing the tracking error. The settling-time parameters T_{c1} and T_{c2} determine the upper bound of the convergence time of the sliding phase and the reaching phase, and they should be chosen according to the requirement of the task. A smaller system convergence time parameter means a larger control torque, so T_{ci} should be selected as large as possible under the premise of meeting the task requirements. For the adaptive law of the controller, when it is difficult to estimate the upper bound of the coupling error of the system, $\hat{b}_{0i}0, \hat{b}_{1i}0$, and $\hat{b}_{2i}0$ $i = 0, 1, 2$ can be defined as 0, and the gain λ_i $i = 0, 1, 2$ affects the update rate of estimated parameters.

4 SIMULATION RESULTS

In this section, to demonstrate the effectiveness of the proposed control scheme, two sets of simulations are considered. Firstly, the predefined-time SMC scheme for a two-link robotic manipulator is considered, and then, the adaptive practical predefined-time SMC scheme for a two-link and a three-DOF robotic manipulator are simulated, respectively.

4.1 Predefined-time SMC for uncertain robotic manipulators

Example 3. Consider a two-link robotic manipulator shown in Figure 4, which is affected by the gravitational field.

The dynamic model parameters of the two-link robotic manipulator are set as:
$l_1 = 1\ \mathrm{m}, l_2 = 0.8\ \mathrm{m}, m_1 = 0.5\ \mathrm{kg}, m_2 = 1.5\ \mathrm{kg}, I_1 = I_2 = 5\ \mathrm{kg\ m^2}$, where l_i, m_i and I_i $i = 1, 2$ are the length, mass, and inertia of link i, respectively, and $g = 9.8\ \mathrm{m/s^2}$ denotes the acceleration due to gravity. Due to the uncertainty of dynamic model, the nominal values of $m_1^0 = 0.6\ \mathrm{kg}, m_2^0 = 0.8\ \mathrm{kg}$, and the nominal values of I_1, I_2 are $I_1^0 = 6\ \mathrm{kg\ m^2}, I_2^0 = 6\ \mathrm{kg\ m^2}$. The disturbances are assumed to

be time-varying and set as $\tau_d = 2\sin t + 0.5\sin 200\pi t, \cos 2t + 0.5\sin 200\pi t^T$. The reference trajectories of robotic manipulator $q_d = {q_{d1}, q_{d2}}^T$ are set as $q_{d1} = 1.25 - \frac{7}{5}\exp(-t) + \frac{7}{20}\exp(-4t), q_{d2} = 1.25 + \exp(-t) - \frac{1}{4}\exp(-4t)$. Simultaneously, the initial states of the two-link robotic manipulator are set as $q_1 0 = -1, q_2 0 = 0, \dot{q}_1 0 = \dot{q}_2 0 = 0$. The parameters of the proposed predefined-time SMCer are $q_1 = 5, q_2 = 1.6, p_1 = 1.1, p_2 = 1.25, \beta_2 = 1, \alpha_1 = 1 / \beta_1 = 4, \alpha_2 = 10^{-3}, s_0 = 0.02, T_{c1} = 1.2, T_{c2} = 0.8$, $b_0 = 9.5, 9.5^T, b_1 = 2.2, 2.2^T, b_2 = 2.8, 2.8^T$.

The simulation results are shown in Figures 5-8. As demonstrated in Figures 5 and 6, the proposed controller can achieve the excellent displacement and velocities tracking performance of link 1 and 2. The displacement tracking errors e_1 and e_2 are shown in Figure 7, from which it is clear that the displacement tracking errors can converge to zero after a short transient. The results of controlling torque in Figure 8 indicate that the system exhibits more pronounced chattering. This is primarily caused by the overestimation of the upper bound on the uncertainty regarding coupling of the robotic manipulator. It can be concluded that the proposed predefined-time SMC scheme can achieve the high-precision tracking of the ideal trajectory of the robotic manipulator within a predefined time T_c, and it has a strong robustness to resist external disturbances and modeling uncertainties.

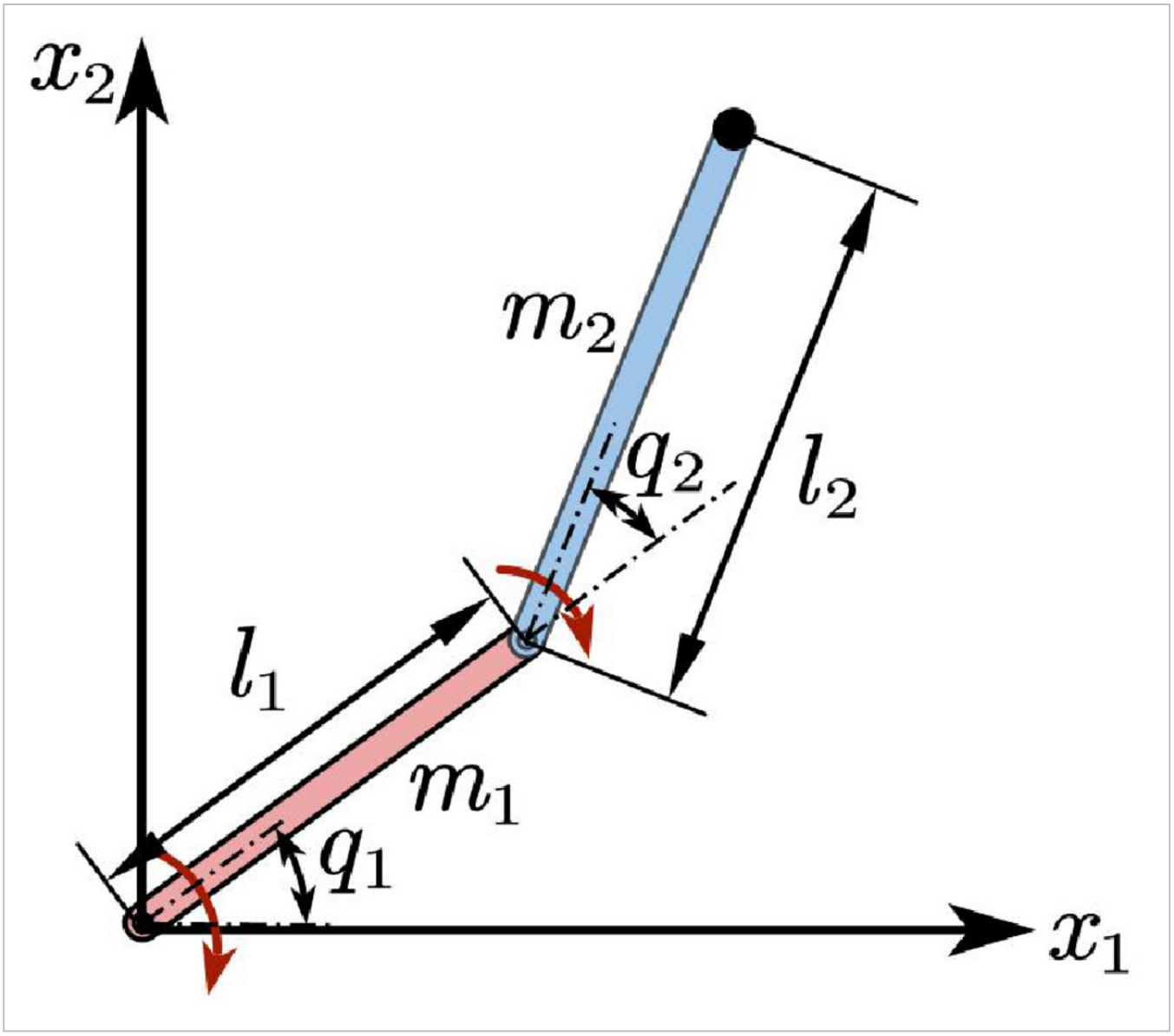

FIGURE 4

Open in figure viewer | PowerPoint

Two-link rigid manipulator schematic.

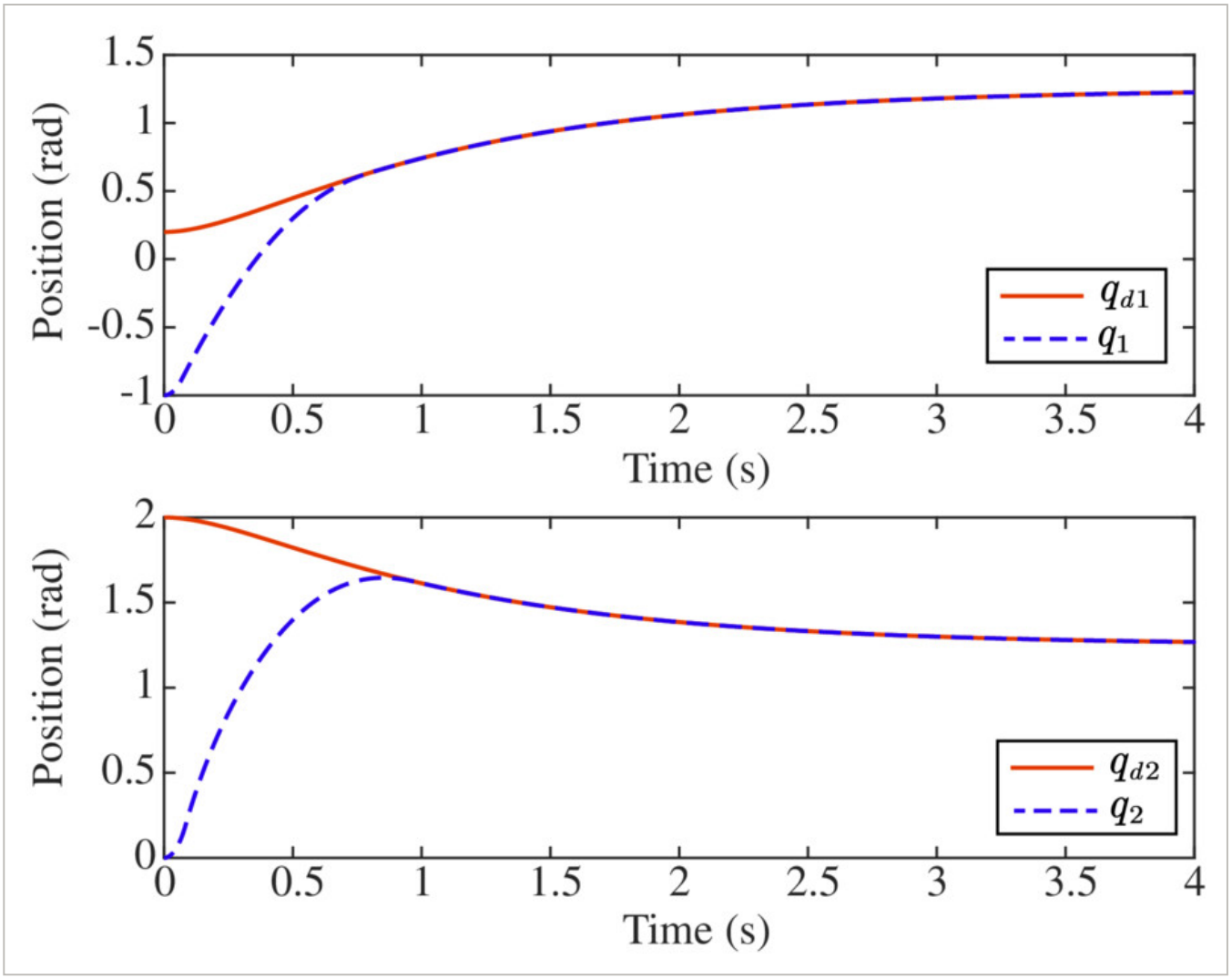

FIGURE 5

Open in figure viewer | PowerPoint

Displacement tracking trajectories.

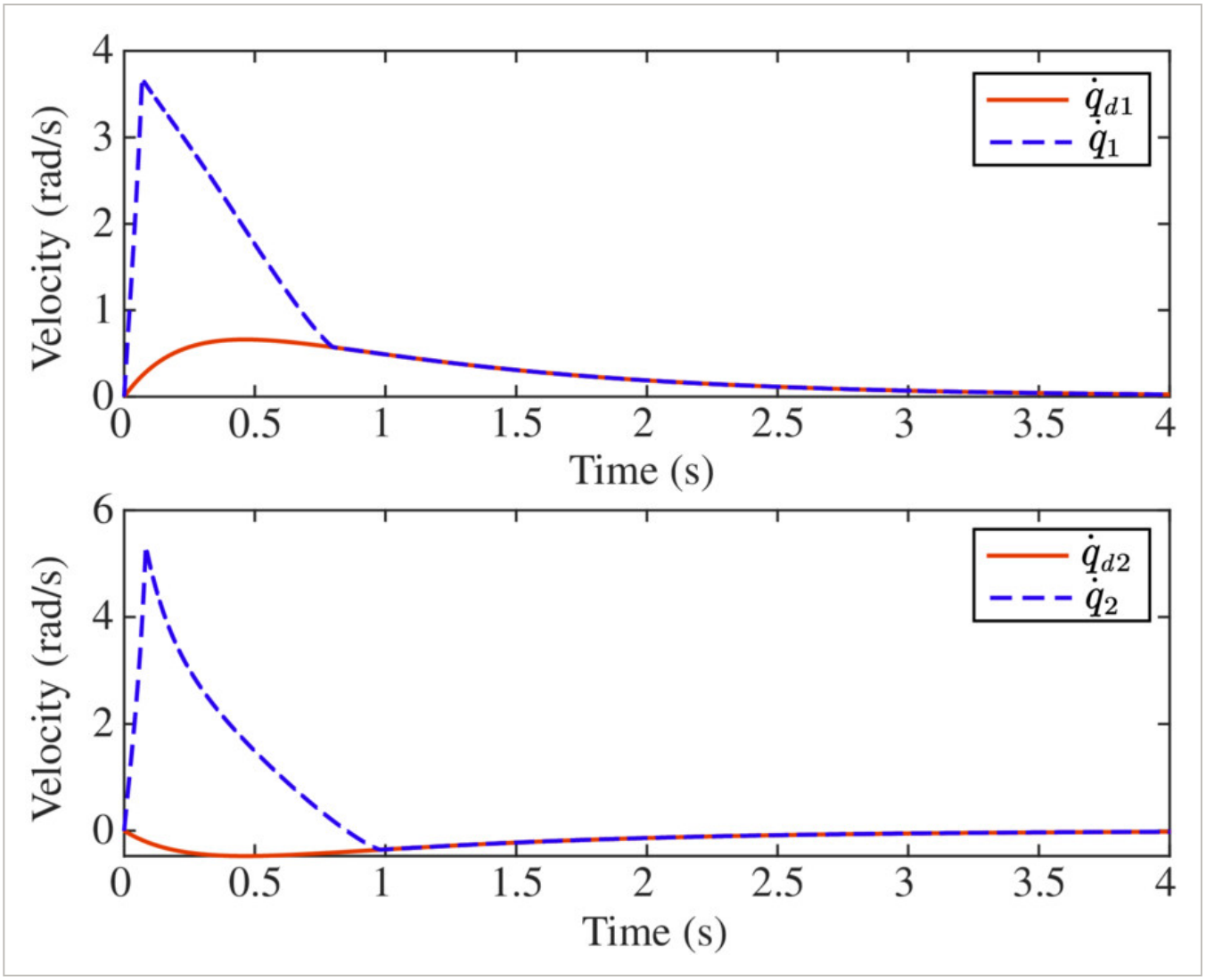

FIGURE 6

Open in figure viewer | PowerPoint

Velocity tracking trajectories.

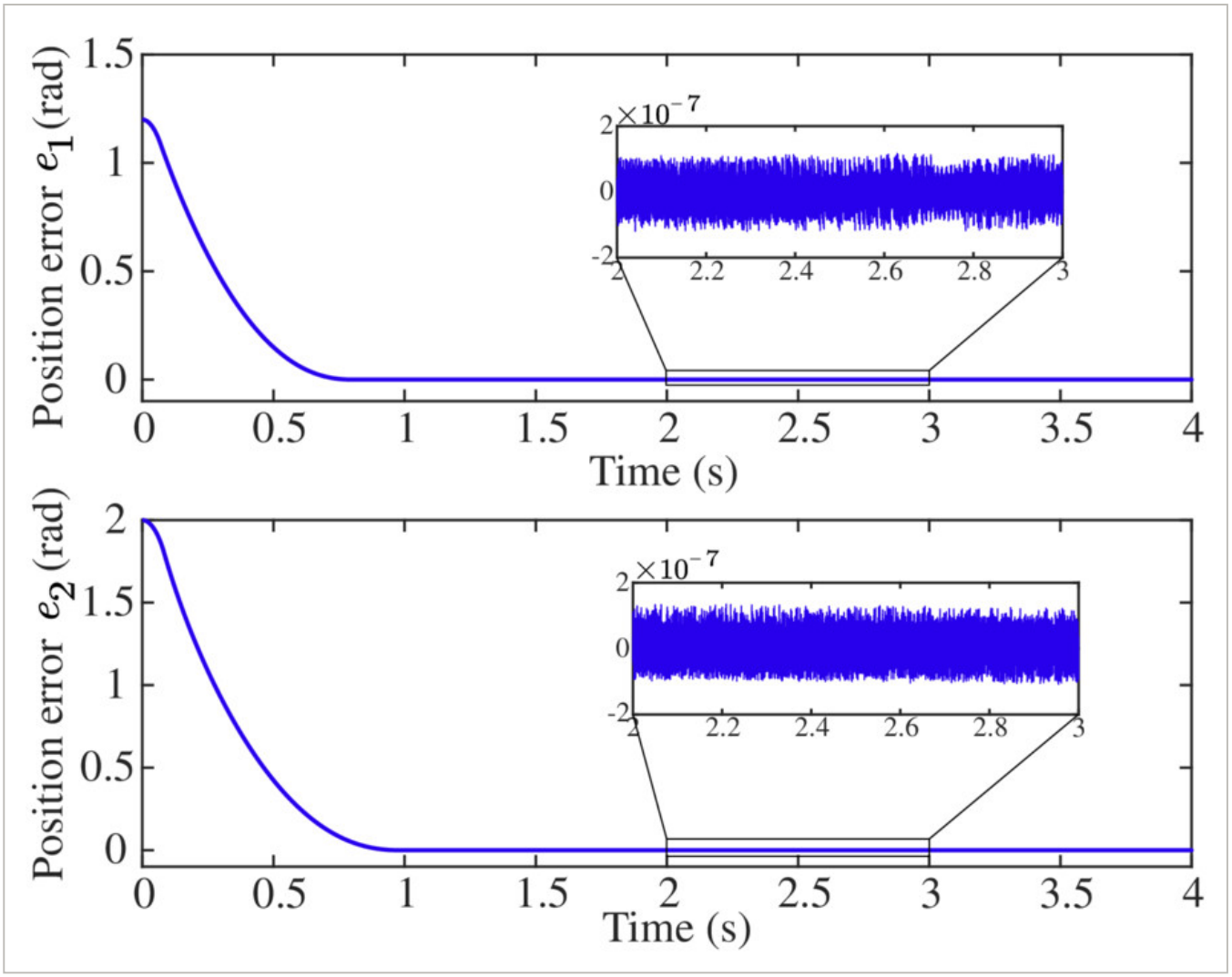

FIGURE 7

Open in figure viewer | PowerPoint

Displacement tracking errors.

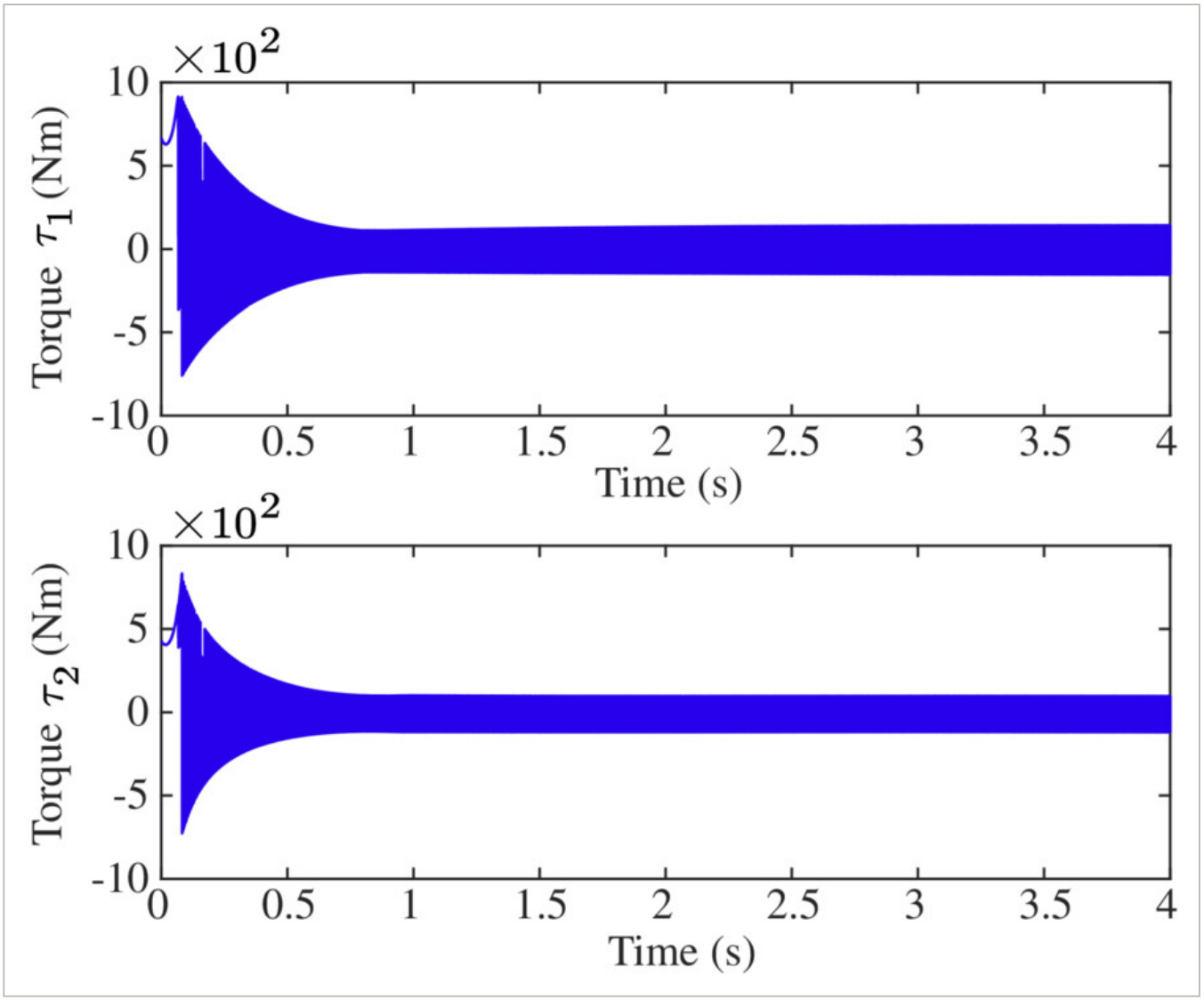

FIGURE 8

Open in figure viewer | PowerPoint

Control torque.

4.2 Adaptive practical predefined-time SMC for uncertain robotic manipulators

In this simulation, the purpose is to show the robustness of the proposed adaptive practical predefined-time SMC scheme with different robotic systems and external disturbances and illustrate the advantages of proposed adaptive control laws. All controller parameters are the same as those in Example 3.

Example 4. Consider the adaptive practical predefined-time SMC algorithm described in Theorem 3, and the initial conditions of adaptive parameters are selected as $\hat{b}_{0i}0 = \hat{b}_{1i}0 = \hat{b}_{2i}0 = 0$ and $\lambda_0 = \lambda_1 = 0.3, \lambda_2 = 0.1$. Then, consider the same two-link robotic manipulator as described in Section 9, and utilize the same reference trajectories and disturbances. Simulation results of tracking performances are shown in Figures 9-13. Figures 9 and 10 show the responses of attitude q and joint velocity $\dot{q}$. Figure 11 shows the displacement

tracking errors of links 1 and 2. Relative to a nonadaptive predefined-time sliding mode controller Example 3, the accuracy of the tracking error is significantly improved. According to Figure 12, the control torques are smooth, which clearly indicates that the proposed adaptive predefined-time sliding mode controller is robust against unknown parameter variations and external disturbances, even if the system uncertainty bound is a priori unknown. All estimated parameters quickly converge to constant values in Figure 13, signifying that the adaptively updated parameters enable the sliding mode surface to converge to zero from any initial state. In summary, the proposed practical adaptive predefined-time SMC scheme enables convergent control of robotic manipulators regardless of the level of coupling uncertainty. Additionally, the controller provides high steady-state tracking performance despite the presence of model uncertainties and disturbances. Furthermore, the proposed scheme results in smooth control torques that reduce system chattering. The combination of these factors makes the proposed scheme a viable solution for achieving precise and stable control of robotic manipulators under uncertain conditions.

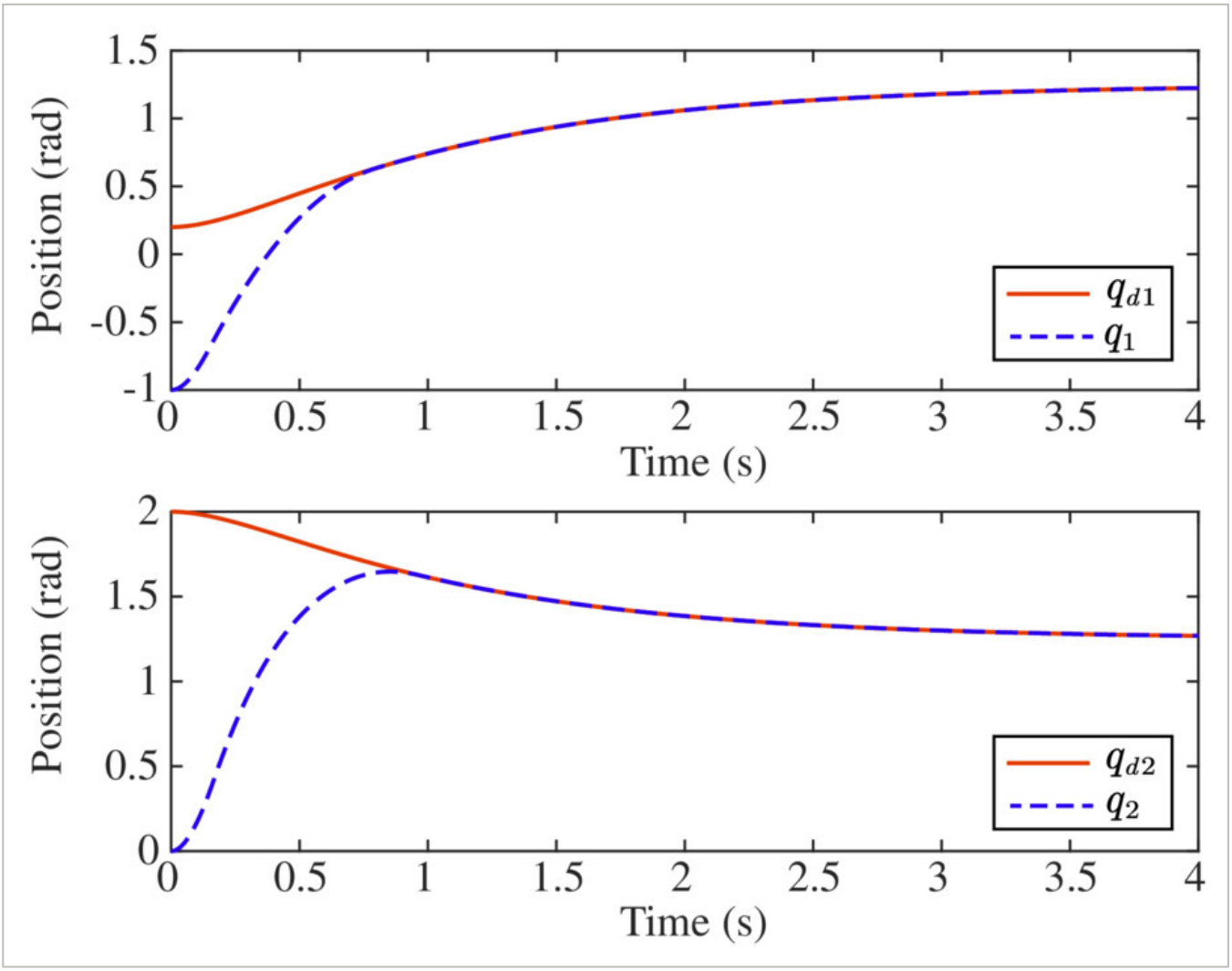

FIGURE 9

Open in figure viewer | PowerPoint

Displacement tracking trajectories.

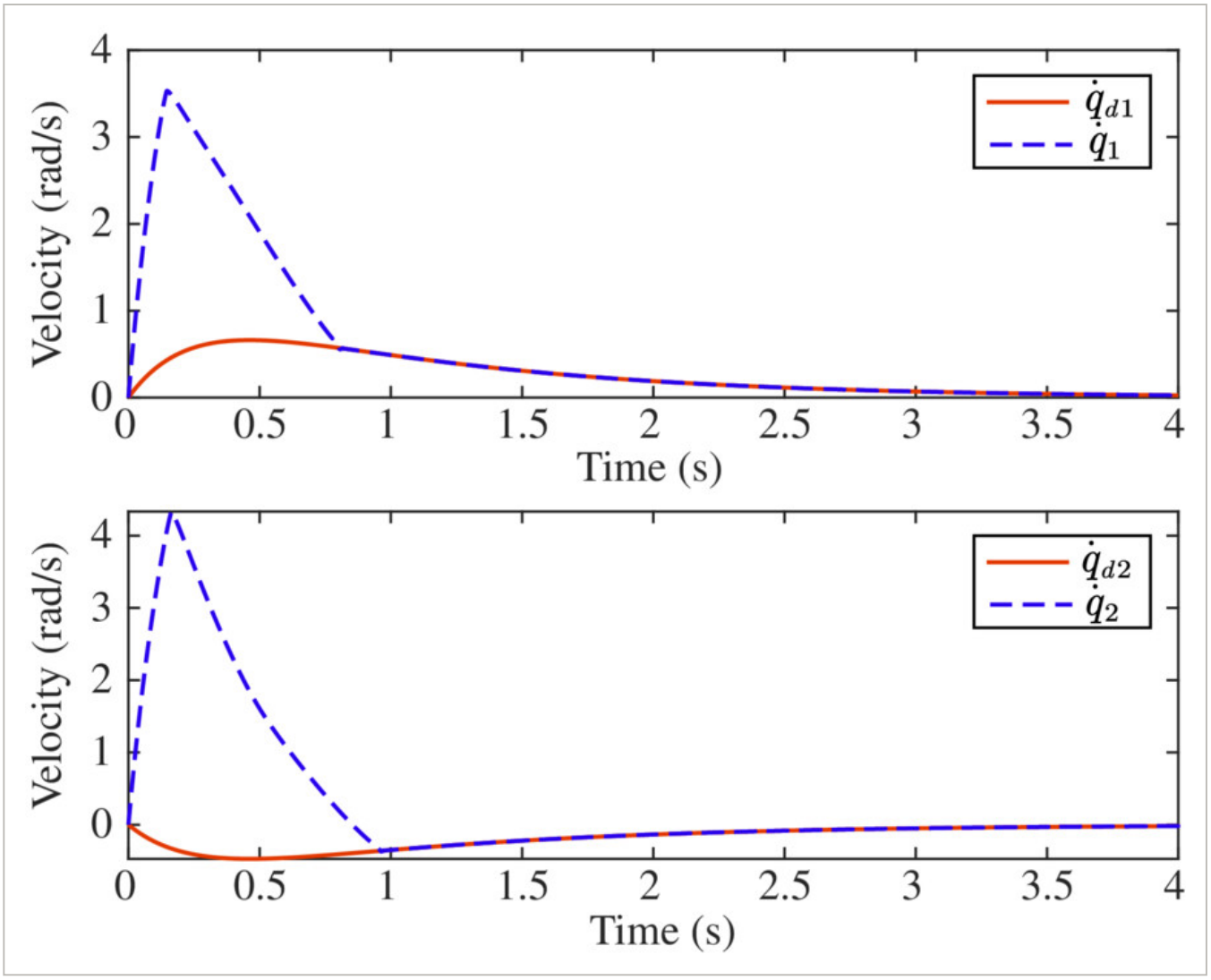

FIGURE 10

Open in figure viewer | PowerPoint

Velocity tracking trajectories.

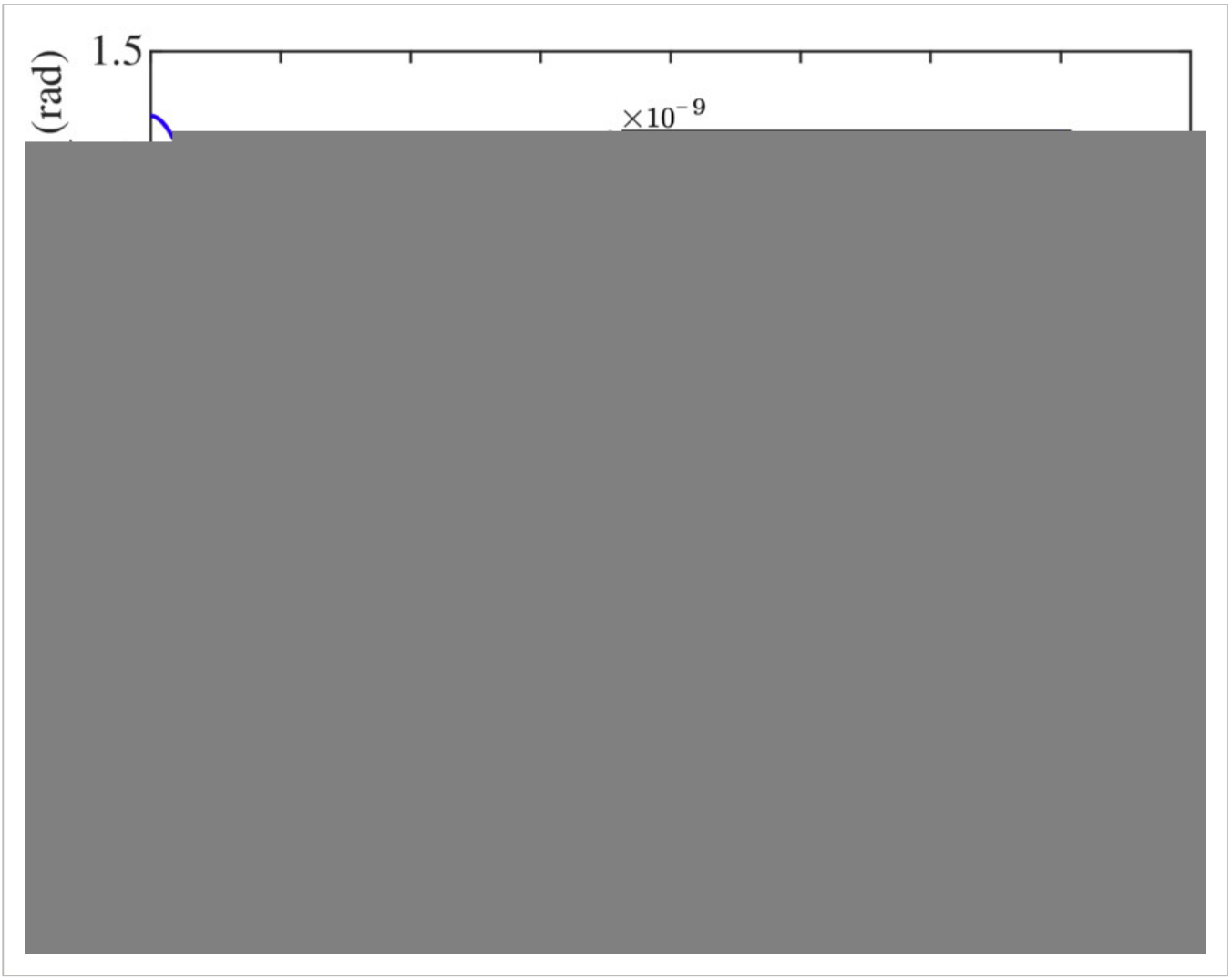

FIGURE 11

Open in figure viewer | PowerPoint

Displacement tracking errors.

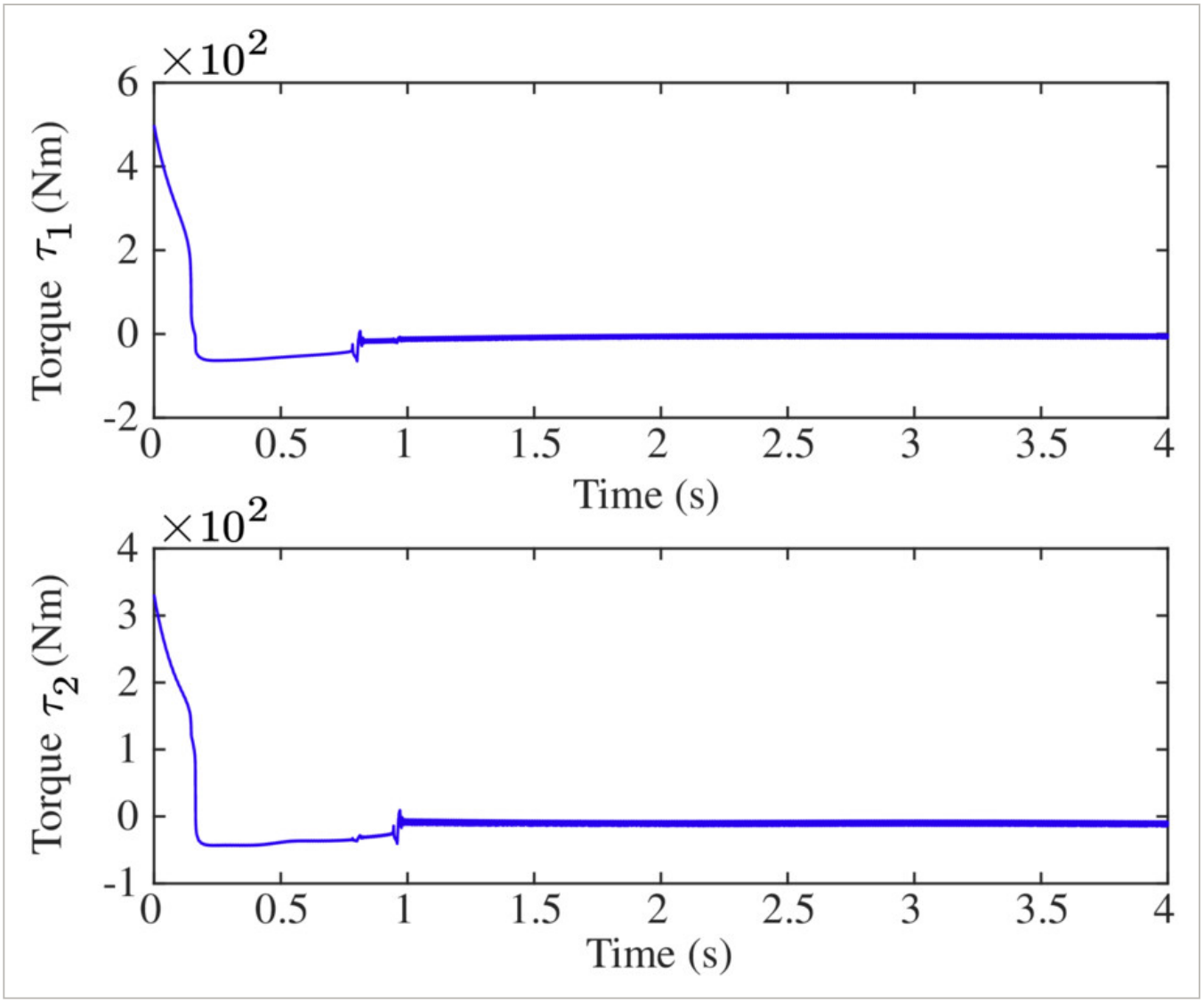

FIGURE 12

Open in figure viewer | PowerPoint

Control torque.

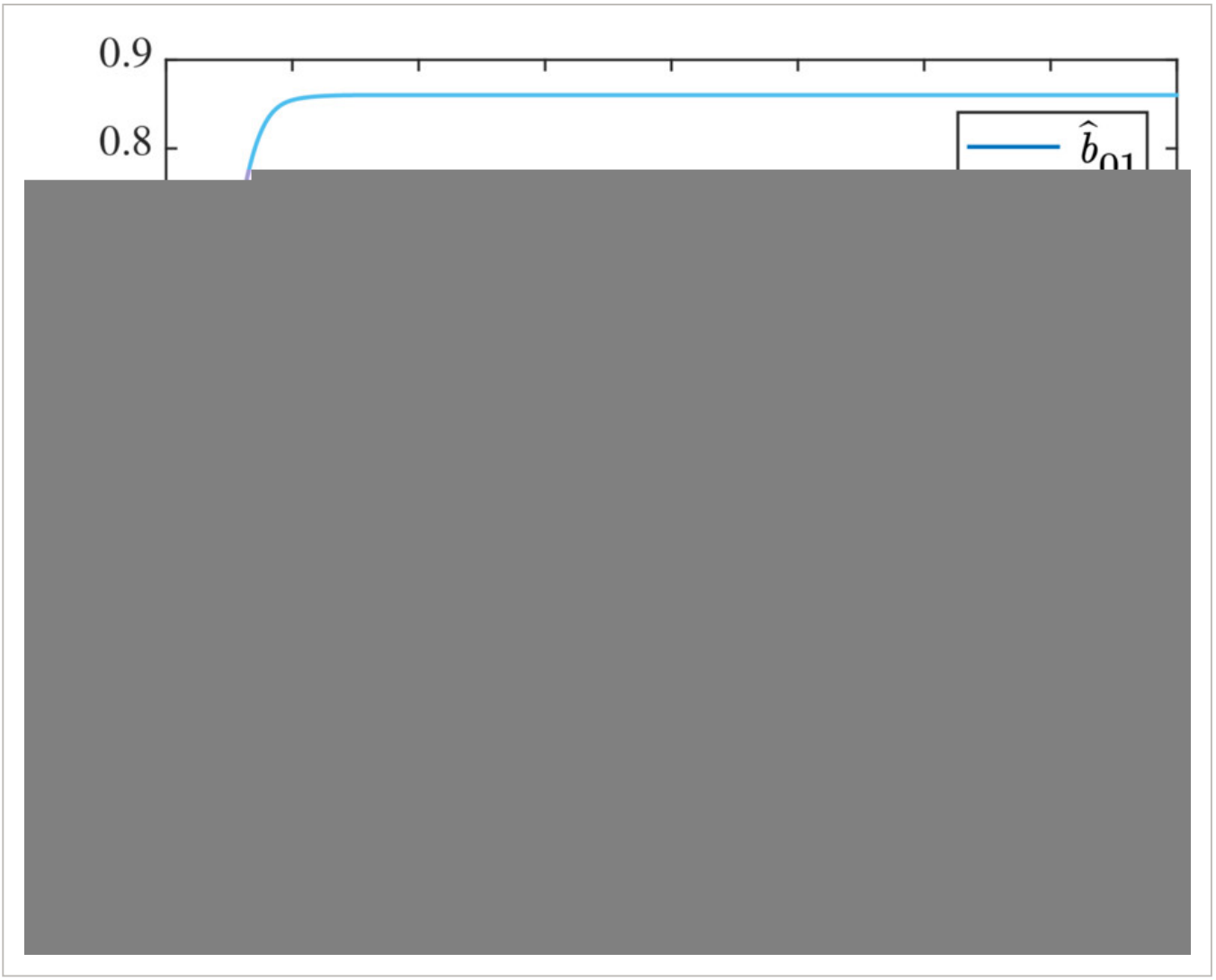

FIGURE 13

Open in figure viewer | PowerPoint

Parameter estimation.

Example 5. In order to demonstrate the robustness of the proposed scheme under different disturbances, monotonically increasing and larger values of time-varying external disturbances are applied to the tracking control of the robotic manipulator. When $t \leqslant 0.5$ s, a monotonically increasing disturbance $\tau_d = 10t, 10t^T$ is applied, and when $t > 0.5$ s, a time-varying disturbance $\tau_d = 5\sin 20\pi t, 5\cos 20\pi t^T$ is considered. Compared with the above-mentioned examples, the disturbances in this example are more complicated, and the same model uncertainties and the control parameters as those in the above-mentioned examples are also considered. Figure 14 shows the displacement tracking errors of links 1 and 2, from which we can obtain that the robotic manipulator can achieve high-precision and fast position tracking of the ideal trajectories. Hence, even considering more complex coupling uncertainties, the robotic manipulator can still guarantee satisfactory trajectory tracking performance with the proposed controller.

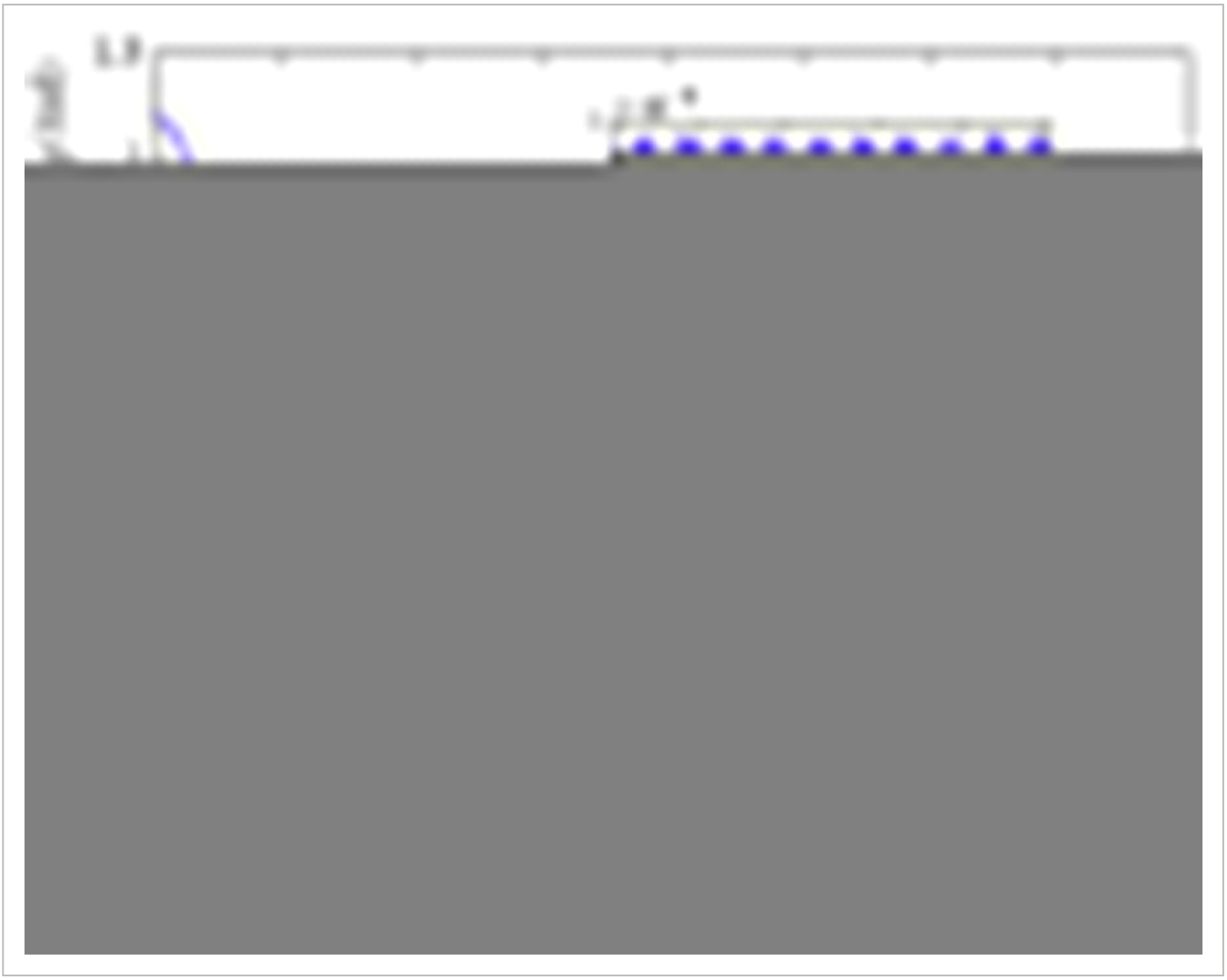

FIGURE 14

Open in figure viewer | PowerPoint

Displacement tracking errors.

Example 6. To further test the feasibility of the proposed control scheme for robotic manipulators with different structures, a 3-DOF robotic manipulator[46] shown in Figure 15 is utilized. The robotic manipulator includes two rotary joints and a prismatic joint, and the two rotation angles of rotary joints are defined as q_1 and q_2, and the translational of the prismatic joint is defined as q_3. The definitions of $Mq, Cq, \dot{q}, Gq$ in dynamic model of robotic manipulator are the same as the work of He et al.[46] Model parameters are chosen as $l_1 = 0.3\ \mathrm{m}, l_2 = 0.4\ \mathrm{m}$, $m_1 = 2\ \mathrm{kg}, m_2 = 2\ \mathrm{kg}, m_3 = 1\ \mathrm{kg}$. The initial states are set as $q_1 0 = 1, q_2 0 = 0$, $q_3 0 = 0.8, \dot{q}_1 0 = \dot{q}_2 0 = \dot{q}_3 0 = 0$, and the reference trajectories are set as $q_d = 1.4\sin 2t, 1.4\cos 2t, \sin 2t^T$. The bounded time-varying disturbances are defined as $\tau_d = \sin 10t + 1, 2\cos 10t + 0.5, 2\sin 10t + 1^T$. Additionally, all the control parameters are chosen as those in Example 4. Figures 16-19 present the performance of 3-DOF robotic manipulator tracking control. From Figures 16 and 17, it can be seen that the system states converge to the ideal trajectories quickly and achieve a good tracking performance. Figures 18 and 19 depict the position tracking error and control torque of the robotic manipulator, respectively. These results

demonstrate the exceptional tracking performance and robustness of the designed control approach for various robotic manipulator models when subject to external disturbances and parameter uncertainties.

FIGURE 15

Open in figure viewer | PowerPoint

3-DOF robotic manipulator architecture.

FIGURE 16

Open in figure viewer | PowerPoint

Displacement tracking trajectories.

FIGURE 17

Open in figure viewer | PowerPoint

Velocity tracking trajectories.

FIGURE 18

Open in figure viewer | PowerPoint

Displacement tracking errors.

FIGURE 19

Open in figure viewer | PowerPoint

Control torque.

5 COMPARATIVE STUDY AND DISCUSSION

To demonstrate the advantages of the proposed adaptive practical predefined-time control scheme, some existing SMC schemes, such as the nonsingular fast terminal SMC (NFTSMC),[47] fixed-time terminal SMC (Fixed TSMC),[10] and the second-order predefined-time SMC algorithm (SOPSMC)[20] are used for comparison. Consider the robotic manipulator and external disturbances in Example 3, and to make the comparison more obvious, the initial positions of the system are set as $q_1 0 = -1$ and $q_2 0 = 0$. In order to ensure a fair comparison, we selected the controller parameters from the references and adjusted the gain parameters to maintain a consistent range of control torque. The selected control parameters are presented in Table 1.

TABLE 1. Simulation parameters of the Fixed TSMC, NFTSMC, and SOPSMC.

Controller	Parameters
Fixed TSMC	$\delta = 0.01, p = 0.5, q = 1.2, r = 1.2, k = 1, K_0 = \text{diag}5, 5, K_1 = \text{diag}10, 10, K_2 = \text{diag}10, 10, b_0 = 12, b_1$
NFTSMC	$\Gamma_1 = \text{diag}5, 5, \Gamma_2 = \text{diag}5/3, 5/3, M_1 = 1, M_2 = 2, b_0 = 12, b_1 = 2.2, b_2 = 2.8$
SOPSMC	$k = 0, T_{c0} = 0.5, T_{c1} = 1, T_{c2} = 1, m_0 = m_1 = m_2 = 1, q_0 = q_2 = 0.5, q_1 = 0.3$

The results of the comparison are shown in Figures 20-23. It is evident from Figures 20-22 that the proposed control scheme exhibits a quicker trajectory tracking rate when compared to finite-time SMC such as NFTSMC and fixed-time SMC such as Fixed TSMC. Additionally, the proposed control scheme has a slower error convergence time than SOPSMC scheme with $T_c = T_{c0} + T_{c1} + T_{c2} = 2.5$. Figure 23 shows that the proposed controller applies a lower control torque than SOPSMC, due to its less conservative settling time. Table 2 lists some quantitative measures, including the convergence time (t_s), steady-state error (ρ_e), maximum control torque ($\tau_{\max}$), integrated absolute error represented by the IAE= $\sum_{k=1}^{N} e_k$, and energy of control input given by ECI= $\sum_{k=1}^{N} {\tau_k}^2$. Numerical comparison results show that the proposed control scheme has a faster error convergence rate than Fixed TSMC and NFTSMC, in the cases where an approximate control torque range exists for joint 1 but a smaller torque range is used for joint 2. The proposed control scheme achieved a higher tracking accuracy than all other control schemes, despite consuming more energy than Fixed TSMC and NFTSMC. It is important to note that the SOPSMC scheme requires a significantly larger torque range than the other control schemes due to its conservative settling time, making it impractical for real-world robotic manipulators.

FIGURE 20

Open in figure viewer | PowerPoint

Displacement tracking trajectories.

FIGURE 21

Open in figure viewer | PowerPoint

Displacement tracking errors.

FIGURE 22

Open in figure viewer | PowerPoint

Velocity tracking errors.

FIGURE 23

Open in figure viewer | PowerPoint

Control torque.

TABLE 2. The performance of the different control schemes.

	Joint 1					Joint 2		
Controller	t_s(s)	e_ρ(rad)	$\tau_{\max}$(Nm)	IAE	ECI	t_s(s)	e_ρ(rad)	$\tau_{\max}$(Nm)
proposed	0.80	5×10^{-9}	499	9.27×10^{-6}	1.95×10^{8}	0.99	8×10^{-9}	331
Fixed TSMC	2.13	5×10^{-6}	463	0.0278	4.85×10^{7}	2.15	4×10^{-6}	647
NFTSMC	2.87	3×10^{-7}	423	0.0022	4.20×10^{7}	3.10	6×10^{-8}	717
SOPSMC	0.72	7×10^{-5}	1.31×10^{4}	0.3215	5.07×10^{9}	0.81	6×10^{-5}	1.14×10

More existing SMC schemes with different convergence time characteristics are compared in Table 3, respectively. According to Table 3, the novelty of the proposed control scheme is emphasized as follows.

(i) Compared to the existing finite-time SMC schemes, the proposed control scheme has its settling time limit only determined by its tunable parameters. This means that the system can determine its maximum settling time without considering the initial state. As a result, our

approach is more suitable for situations where it is challenging to obtain the initial state, and where it is essential to have the system state converge quickly.

(ii) The proposed predefined-time SMC scheme differs from existing fixed-time SMC schemes. The tunable parameters directly determine the limit of settling time, whereas the settling time in fixed-time SMC relies on the complex function of system parameters. This means that the relationship between fixed-time stabilization and controller parameters is not explicit. Furthermore, regarding the fixed-time SMC schemes in Table 3,[8, 10, 48] their fixed-time stability derivation relies on the settling time function introduced by Polyakov.[5] However, the upper bound condition used for estimating the settling-time bound is too conservative, leading to the waste of control energy and potentially exceeding the system's control input limit.

(iii) In contrast to existing predefined-time SMC schemes, this paper extends the strong predefined-time stability to second-order nonlinear systems with a nonconservative upper bound on settling time. Our approach achieves strong predefined-time convergence for second-order systems when the uncertainty of the system is not considered. Moreover, the sliding mode surface introduced by Sánchez-Torres[18] experiences an "exponential explosion", creating significant control input ranges for the system. In contrast, our approach overcomes this limitation, achieving smaller control inputs than existing predefined-time control schemes.

TABLE 3. Comparison of proposed control scheme with some existing SMC schemes.

Reference	Settling time/ comparison to ours	Orders of system	Whether it is necessary to provide an upper bound of uncertainty?
49	Infinite-time	Second-order	None provided. Based on time-delay estimation technique.
47	Finite-time	First-order and second-order	Yes
37	Finite-time	Second-order	None provided. Based on adaptive laws with more defined parameters
50	Finite-time	Second-order	None provided. Based on neural networks
8, 48	Fixed-Time	Second-order	Yes
10	Approximate fixed-time	Second-order	Yes
13-16, 21	Predefined-time. More conservation	First-order	Yes
24	Predefined-time. More conservation	High-order	Disturbance not considered

Reference	Settling time/ comparison to ours	Orders of system	Whether it is necessary to provide an upper bound of

Apart from the aforementioned benefits, the proposed adaptive control approach offers key benefits when dealing with model uncertainty and external disturbances, as it is designed to function independently of knowledge regarding the upper bounds of system coupling uncertainty. This means that the proposed control method not only prevents disturbances from being overestimated but also mitigates system chattering. Additionally, numerical simulations confirm that the method is robust to different robotic systems and varying degrees of external disturbances.

6 CONCLUSION

In this work, a nonconservative predefined-time SMC scheme and an adaptive practical predefined-time SMC scheme have been presented for uncertain robotic manipulators. On the one hand, a predefined-time SMCer for a class of second-order system is designed, which has a nonconservative upper bound for settling time. In the case of without considering disturbances, the proposed controller can achieve strong predefined-time convergence of the second-order system, and it is proved by the Lyapunov stability theorem. On the other hand, considering the model uncertainty and external disturbance of the robotic manipulator, a practical predefined-time stability criterion and adaptive laws for predefined-time SMCer are designed. In consequence, the upper bound of the coupling uncertainty is not required in the procedure of the controller design, and the proposed controller has a strong robustness to different robotic manipulators and external disturbances. Several numerical simulation results have highlighted the effectiveness of the proposed scheme in terms of the tracking control of the robotic manipulator with the coupling uncertainty. In our future work, we aim to reduce the initial torque of the previously proposed predefined-time controller for trajectory tracking control of a robotic manipulator to ensure that it fulfills actual control requirements and to validate experimentally in real-world scenarios.

FUNDING INFORMATION

This work is supported by the National Natural Science Foundation of China (62235018 and 11972343).

CONFLICT OF INTEREST STATEMENT

The authors declare no potential conflict of interests.

APPENDIX A: THE PROOF OF LEMMA 3

Proof. Considering a constant $0 < \phi < 1$, (5) can be written as

$$\dot{V}x \leqslant -\phi\xi \exp\alpha V x^{p} V x^{\beta q} - 1 - \phi\xi \exp\alpha V x^{p} V x^{\beta q} + \eta, \quad \text{(A1)}$$

where $\xi = \frac{\alpha^{\frac{\beta q-1}{p}}\Gamma\frac{1-\beta q}{p}}{pT_c}$.

If $Vx > \frac{\eta}{\phi\xi\alpha}^{\frac{1}{p+\beta q}}$, taking the logarithm of both sides simultaneously yields

$$p + \beta q \ln Vx > \ln\frac{\eta}{\phi\xi\alpha}. \tag{A2}$$

Then, (A2) can be further written as

$$Vx^{p}Vx^{\beta q} > \frac{\eta}{\phi\xi\alpha}. \tag{A3}$$

Considering $e^{x} \geqslant x + 1 > x$, (A3) can be obtained that

$$\frac{\eta}{\phi\xi} < \alpha Vx^{p}Vx^{\beta q} < \exp\alpha Vx^{p}Vx^{\beta q}. \tag{A4}$$

Due to the fact that $\eta < \phi\xi\exp\alpha Vx^{p}Vx^{\beta q}$, (A1) can be further written as

$$\dot{V}x \leqslant -1 - \phi\xi\exp\alpha Vx^{p}Vx^{\beta q}. \tag{A5}$$

According to Lemma 1, it shows that the solution of system (1) is practically predefined-time stable with the predefined time $\frac{T_c}{1-\phi}$ and converge to the compact set

$$x \in Vx \leqslant \frac{\eta}{\phi\xi\alpha}^{\frac{1}{p+\beta q}}. \tag{A6}$$

This completes the proof of Lemma 3.

APPENDIX B: DERIVATION OF THE REDUCED-ORDER DYNAMICS

Proof. When the system state convergence enters the sliding phase once $s = 0$, the sliding mode surface in (14) can be written as

$$-x_2 = \left| \mid x_2 \mid^{2} \operatorname{sign} x_2 + \frac{2\gamma_1^2}{T_{c1}^2}\alpha_1 \mid x_1 \mid^{p_1} + \beta_1 \mid x_1 \mid^{q_1} \operatorname{sign} x_1 \right|^{\frac{1}{2}}. \tag{B1}$$

Then, taking square on both sides of the (B1), it has

$$x_2^2 = \mid x_2^2 \operatorname{sign} x_2 + \frac{2\gamma_1^2}{T_{c1}^2}\alpha_1 \mid x_1 \mid^{p_1} + \beta_1 \mid x_1 \mid^{q_1} \operatorname{sign} x_1 \mid . \tag{B2}$$

If $x_2 \geqslant 0$, with $\alpha_1, \beta_1 > 0$, it is easy to obtain that $x_1 \leqslant 0$ and

$$x_2 = \frac{\gamma_1}{T_{c1}}\alpha_1 \mid x_1 \mid^{p_1} + \beta_1 \mid x_1 \mid^{q_1}{}^{\frac{1}{2}}. \tag{B3}$$

If $x_2 < 0$, with $\alpha_1, \beta_1 > 0$, it can be obtained that $x_1 > 0$ and

$$x_2 = -\frac{\gamma_1}{T_{c1}}\alpha_1 \mid x_1 \mid^{p_1} + \beta_1 \mid x_1 \mid^{q_1} \frac{1}{2}. \tag{B4}$$

Therefore, with (B3) and (B4), the solution of system (12) can be written as

$$\dot{x}_1 = x_2 = -\frac{\gamma_1}{T_{c1}}\alpha_1 \mid x_1 \mid^{p_1} + \beta_1 \mid x_1 \mid^{q_1} \frac{1}{2} \mathrm{sign} x_1. \tag{B5}$$

Open Research

DATA AVAILABILITY STATEMENT

Data sharing not applicable to this article as no datasets were generated or analyzed during the current study.

REFERENCES

1 Adil HMM, Ahmed S, Ahmad I. Control of MagLev system using supertwisting and integral backstepping sliding mode algorithm. *IEEE Access*. 2020; **8**: 51352-51362.

Web of Science® | Google Scholar

2 Sai H, Xu Z, Zhang E, Han C, Yu Y. Chattering-free fast fixed-time sliding mode control for uncertain robotic manipulators. *Int J Control Autom Syst*. 2023; **21**(2): 630-644.

Web of Science® | Google Scholar

3 Drakunov SV, Utkin VI. Sliding mode control in dynamic systems. *Int J Control*. 1992; **55**(4): 1029-1037.

Web of Science® | Google Scholar

4 Zhang L, Liu L, Wang Z, Xia Y. Continuous finite-time control for uncertain robot manipulators with integral sliding mode. *IET Control Theory Appl*. 2018; **12**(11): 1621-1627.

Web of Science® | Google Scholar

5 Polyakov A. Nonlinear feedback design for fixed-time stabilization of linear control systems. *IEEE Trans Autom Control*. 2011; **57**(8): 2106-2110.

Web of Science® | Google Scholar

6 Zuo Z, Tie L. A new class of finite-time nonlinear consensus protocols for multi-agent systems. *Int J Control*. 2014; **87**(2): 363-370.

Web of Science® Google Scholar

7 Zuo Z, Tie L. Distributed robust finite-time nonlinear consensus protocols for multi-agent systems. *Int J Syst Sci*. 2016; **47**(6): 1366-1375.

Web of Science® Google Scholar

8 Zuo Z. Non-singular fixed-time terminal sliding mode control of non-linear systems. *IET Control Theory Appl*. 2015; **9**(4): 545-552.

Web of Science® Google Scholar

9 Dong Y, Chen Z. Fixed-time robust networked observers and its application to attitude synchronization of spacecraft systems. *IEEE Trans Cybern*. 2022.

Web of Science® Google Scholar

10 Su Y, Zheng C, Mercorelli P. Robust approximate fixed-time tracking control for uncertain robot manipulators. *Mech Syst Signal Process*. 2020; **135**(1): 106379.

Google Scholar

11 Sai H, Xu Z, Xia C, Sun X. Approximate continuous fixed-time terminal sliding mode control with prescribed performance for uncertain robotic manipulators. *Nonlinear Dyn*. 2022; **110**(1): 431-448.

Web of Science® Google Scholar

12 Zhang L, Liu H, Tang D, Hou Y, Wang Y. Adaptive fixed-time fault-tolerant tracking control and its application for robot manipulators. *IEEE Trans Ind Electron*. 2021; **69**(3): 2956-2966.

Web of Science® Google Scholar

13 Sánchez-Torres JD, Gómez-Gutiérrez D, López E, Loukianov AG. A class of predefined-time stable dynamical systems. *IMA J Math Control Inf*. 2018; **35**(Supplement_1): i1-i29.

Google Scholar

14 Sánchez-Torres JD, Sanchez EN, Loukianov AG. *Predefined-time stability of dynamical systems with sliding modes*. IEEE; 2015: 5842-5846.

Google Scholar

15 Jiménez-Rodríguez E, Muñoz-Vázquez AJ, Sánchez-Torres JD, Loukianov AG. A note on predefined-time stability. *IFAC-PapersOnLine*. 2018; **51**(13): 520-525.

Google Scholar

16 Jimenez-Rodriguez E, Munoz-Vazquez AJ, Sanchez-Torres JD, Defoort M, Loukianov AG. A Lyapunov-like characterization of predefined-time stability. *IEEE Trans Autom Control*. 2020; **65**(11): 4922-4927.

Web of Science® Google Scholar

17 Jiménez-Rodríguez E, Sánchez-Torres JD, Loukianov A. On optimal predefined-time stabilization. *Int J Robust Nonlinear Control*. 2017; **27**(17): 3620-3642.

Web of Science® Google Scholar

18 Sánchez-Torres JD, Defoort M, Muñoz-Vázquez AJ. *A Second Order Sliding Mode Controller with Predefined-Time Convergence*. IEEE; 2018: 1-4.

Google Scholar

19 Aldana-López R, Gómez-Gutiérrez D, Jiménez-Rodríguez E, Sánchez-Torres JD, Defoort M. Enhancing the settling time estimation of a class of fixed-time stable systems. *Int J Robust Nonlinear Control*. 2019; **29**(12): 4135-4148.

Web of Science® Google Scholar

20 Jiménez-Rodríguez E, Loukianov AG, Sánchez-Torres JD. *A Second Order Predefined-Time Control Algorithm*. IEEE; 2017: 1-6.

Google Scholar

21 Muñoz-Vázquez AJ, Sánchez-Torres JD, Defoort M. Second-order predefined-time sliding-mode control of fractional-order systems. *Asian J Control*. 2020; **24**: 74-82.

Web of Science® Google Scholar

22 Yang XW, Fan XP, Long F, Gr L. Predefined-time robust control with formation constraints and saturated controls. *Nonlinear Dyn*. 2022; **110**(3): 2535-2554.

Web of Science® Google Scholar

23 Trentin JFS, Santos DA. Predefined-time global sliding mode control design for a 3D pendulum. *Nonlinear Dyn*. 2022; **109**(3): 1693-1704.

Web of Science® Google Scholar

24 Jimenez-Rodriguez E, Sanchez-Torres JD, Gomez-Gutierrez D, Loukianov AG. *Predefined-Time Stabilization of High Order Systems*. IEEE; 2017: 5836-5841.

Google Scholar

25 Abadi ASS, Hosseinabadi PA, Mekhilef S, Ordys A. A new strongly predefined time sliding mode controller for a class of cascade high-order nonlinear systems. *Archives Control Sci*. 2020; **30**: 599-620.

Web of Science® Google Scholar

26 Jimenez-Rodriguez E, Sanchez-Torres JD, Gomez-Gutierrez D, Loukianov AG. *Predefined-time tracking of a class of mechanical systems*. IEEE; 2016: 1-5.

Google Scholar

27 Munoz-Vazquez AJ, Sanchez-Torres JD, Jimenez-Rodriguez E, Loukianov AG. Predefined-time robust stabilization of robotic manipulators. *IEEE-ASME Trans Mechatron*. 2019; **24**(3): 1033-1040.

Web of Science® Google Scholar

28 Muñoz-Vázquez AJ, Sánchez-Torres JD. Predefined-time control of cooperative manipulators. *Int J Robust Nonlinear Control*. 2020; **30**(17): 7295-7306.

Web of Science® Google Scholar

29 Muñoz-Vázquez AJ, Sánchez-Torres JD, Gutiérrez-Alcalá S, Jiménez-Rodríguez E, Loukianov AG. Predefined-time robust contour tracking of robotic manipulators. *J Franklin Instit Eng Appl Math*. 2019; **356**(5): 2709-2722.

Web of Science® Google Scholar

30 Obregon-Flores J, Arechavaleta G, Becerra HM, Morales-Diaz A. Predefined-time robust hierarchical inverse dynamics on torque-controlled redundant manipulators. *IEEE Trans Robot*. 2021; **37**(3): 962-978.

Web of Science® Google Scholar

31 Pal AK, Kamal S, Nagar SK, Bandyopadhyay B, Fridman LM. Design of controllers with arbitrary convergence time. *Automatica*. 2020; **112**(112): 108710.

Google Scholar

32 Gómez-Gutiérrez D. On the design of nonautonomous fixed-time controllers with a predefined upper bound of the settling time. *Int J Robust Nonlinear Control*. 2020; **30**(10): 3871-3885.

Web of Science® | Google Scholar

33 Fang H, Wu Y, Xu T, Wan F. Adaptive neural sliding mode control of uncertain robotic manipulators with predefined time convergence. *Int J Robust Nonlinear Control*. 2022; **32**(17): 9213-9238.

Web of Science® | Google Scholar

34 Sun Y, Gao Y, Zhao Y, et al. Neural network-based tracking control of uncertain robotic systems: predefined-time nonsingular terminal sliding-mode approach. *IEEE Trans Ind Electron*. 2022; **69**(10): 10510-10520.

Web of Science® | Google Scholar

35 Wang Q, Cao J, Liu H. Adaptive fuzzy control of nonlinear systems with predefined time and accuracy. *IEEE Trans Fuzzy Syst*. 2022; **30**(12): 5152-5165.

Web of Science® | Google Scholar

36 Sai H, Xu Z, He S, Zhang E, Zhu L. Adaptive nonsingular fixed-time sliding mode control for uncertain robotic manipulators under actuator saturation. *ISA Trans*. 2022; **123**: 46-60.

PubMed | Web of Science® | Google Scholar

37 Boukattaya M, Mezghani N, Damak T. Adaptive nonsingular fast terminal sliding-mode control for the tracking problem of uncertain dynamical systems. *ISA Trans*. 2018; **77**: 1-19.

PubMed | Web of Science® | Google Scholar

38 Sánchez-Torres JD, Muñoz-Vázquez AJ, Defoort M, Aldana-López R, Gómez-Gutiérrez D. Predefined-time integral sliding mode control of second-order systems. *Int J Syst Sci*. 2020; **51**(16): 3425-3435.

Web of Science® | Google Scholar

39 Sánchez-Torres JD, Defoort M, Muñoz-Vázquez AJ. Predefined-time stabilisation of a class of nonholonomic systems. *Int J Control*. 2020; **93**(12): 2941-2948.

Web of Science® | Google Scholar

40 Spong MW, Hutchinson S, Vidyasagar M, others. *Robot modeling and control. 3*. Wiley; 2006.

Google Scholar

41 Li P, Ma J, Zheng Z. Robust adaptive sliding mode control for uncertain nonlinear MIMO system with guaranteed steady state tracking error bounds. *J Franklin Instit Eng Appl Math*. 2016; **353**(2): 303-321.

Web of Science® | Google Scholar

42 Yi S, Zhai J. Adaptive second-order fast nonsingular terminal sliding mode control for robotic manipulators. *ISA Trans*. 2019; **90**: 41-51.

PubMed | Web of Science® | Google Scholar

43 Neila MB, Tarak D. Adaptive terminal sliding mode control for rigid robotic manipulators. *Int J Autom Comput*. 2011; **8**(2): 215-220.

Google Scholar

44 Zhihong M, O'day M, Yu X. A robust adaptive terminal sliding mode control for rigid robotic manipulators. *J Intell Robot Syst*. 1999; **24**(1): 23-41.

Web of Science® | Google Scholar

45 Liu C, Zhao Z, Wen G. Adaptive neural network control with optimal number of hidden nodes for trajectory tracking of robot manipulators. *Neurocomputing*. 2019; **350**: 136-145.

Web of Science® | Google Scholar

46 He W, Huang H, Ge SS. Adaptive neural network control of a robotic manipulator with time-varying output constraints. *IEEE Trans Syst Man Cybern*. 2017; **47**(10): 3136-3147.

Google Scholar

47 Yang L, Yang J. Nonsingular fast terminal sliding-mode control for nonlinear dynamical systems. *Int J Robust Nonlinear Control*. 2011; **21**(16): 1865-1879.

Web of Science® | Google Scholar

48 Li H, Cai Y. On SFTSM control with fixed-time convergence. *IET Control Theory Appl*. 2017; **11**(6): 766-773.

Web of Science® | Google Scholar

49 Baek J, Jin M, Han S. A new adaptive sliding-mode control scheme for application to robot manipulators. *IEEE Trans Ind Electron*. 2016; **63**(6): 3628-3637.

Web of Science® | Google Scholar

50 Jia S, Shan J. Finite-Time Trajectory Tracking Control of Space Manipulator Under Actuator Saturation. *IEEE Trans Ind Electron*. 2020; **67**(3): 2086-2096.

Web of Science® | Google Scholar

51 Jimenez-Rodriguez E, Sanchez-Torres JD, Munoz-Vazquez AJ, Defoort M, Loukianov AG. *A Class of Predefined-Time Stabilizing Controllers for Nonholonomic Systems*. IEEE; 2019: 464-471.

Google Scholar